NASA
Technical
Paper
2595 Revised

February 1988

Landsat-4 and Landsat-5 Multispectral Scanner Coherent Noise Characterization and Removal

James C. Tilton
and William L. Alford

(NASA-TP-2595-Rev) LANDSAT-4 AND LANDSAT-5 MULTISPECTRAL SCANNER COHERENT NOISE CHARACTERIZATION AND REMOVAL (NASA) 46 p CSCL 08B
N89-12114
Unclas
H1/43 0174780

NASA

NASA Technical Paper 2595 Revised

1988

Landsat-4 and Landsat-5 Multispectral Scanner Coherent Noise Characterization and Removal

James C. Tilton
and William L. Alford

Goddard Space Flight Center
Greenbelt, Maryland

National Aeronautics
and Space Administration

Scientific and Technical Information Division

All measurement values are expressed in the International System of Units (SI) in accordance with NASA Policy Directive 2220.4, paragraph 4.

CONTENTS

	Page
INTRODUCTION	1
LANDSAT MSS SAMPLING SCHEMA	4
CHARACTERIZING THE NOISE	4
NOISE CHARACTERIZATION RESULTS	5
FILTERING LANDSAT-4 MSS COHERENT NOISE	8
RETROFIT OF LANDSAT-D ′ TO REMOVE COHERENT NOISE	9
CONCLUDING REMARKS	12
REFERENCES	13
APPENDIX A - CHARACTERIZATION AND REMOVAL OF COHERENT NOISE FROM LANDSAT MSS IMAGERY DATA USING THE IDIMS FACILITY AT THE NASA GODDARD SPACE FLIGHT CENTER	A-1
APPENDIX B - FOURIER MAGNITUDE PLOTS OF RESEQUENCED DATA FROM THE LANDSAT MSS COHERENT NOISE CHARACTERIZATION STUDY	B-1
APPENDIX C - DETAILED LOOK AT THE RESULTS FROM THE LANDSAT MSS COHERENT NOISE STUDY	C-1
APPENDIX D - PLOTS OF FILTERS USED IN FILTERING LANDSAT-4 MSS COHERENT NOISE FROM THE NORTH CAROLINA DATA SET	D-1

LANDSAT-4 AND LANDSAT-5 MULTISPECTRAL SCANNER COHERENT NOISE CHARACTERIZATION AND REMOVAL

James C. Tilton
William L. Alford*
Space Data and Computing Division
Goddard Space Flight Center
Greenbelt, Maryland

INTRODUCTION

A coherent noise pattern is present in Landsat-4 Multispectral Scanner (MSS) imagery. A typical example of the noise pattern is shown in Figure 1a. The structure of the noise pattern can be seen more clearly by filtering out the noise pattern (using a technique developed in this paper) and displaying the difference image between the original and filtered images. Figure 1b is the filtered version of Figure 1a, and Figure 1c is the difference image. A constant bias was added to the difference image to produce a displayable positive image.

Figure 1c shows that the coherent noise appears in the imagery as an oscillating noise pattern with a period of approximately three to four pixels running roughly diagonal from NNE to SSW. The oscillating noise pattern exhibits an irregular phase shift between groups of lines. This noise pattern can be detected most clearly in the original image over uniform areas such as bodies of water, and can be seen most easily if the image radiance values are stretched to fully use the dynamic range of the display device (as was done in Figure 1). The noise pattern has a maximum magnitude of plus or minus three counts. In the difference image (disregarding the bias), some 58 percent of the pixels have value 0 (i.e., 58 percent of the pixels in the original and filtered images are identical); some 40 percent of the pixels have value ± 1; approximately 2 percent of the pixels have value ± 2, and less than 0.01 percent of the pixels have value ± 3. The variance of the difference image (in each band) is approximately 0.5.

A comprehensive study of the effect of this noise pattern on the results obtained from various image analysis techniques has not been carried out. However, the noise pattern is apparently strong enough to affect analysis results. An idea of this effect can be obtained by clustering a section of original data, and comparing the resulting cluster map to one obtained by clustering a filtered version of the same section of data. The ISOCLAS function was used to cluster the original data shown in Figure 1a, and the filtered data shown in Figure 1b. Sixteen clusters were specified in both cases. Color-coded maps of the resulting clusters are displayed in Figures 2a and 2b. The original data produces four water clusters, whereas the filtered data produce only one water cluster. The land clusters are also perturbed by the presence of the coherent noise.

The ISOCLAS function was run with a set of parameters commonly used by analysts at the National Aeronautic and Space Administration (NASA) Goddard Space Flight Center (GSFC) for this type of data.† No attempt was made to adjust the parameters to minimize or maximize the unreasonable clusters caused by the noise in the data. Another clustering program, or ISOCLAS run with a different set of parameters, might not produce such a pronounced effect from the noise, or may even produce a more pronounced effect. At least one case of the noise effect has caused major problems for a research project: the noise effect causes classification errors between ocean and wetlands in a study of ocean intrusion over time along the Louisiana coast (Nelson May, personal communication, Center for Wetland Resources, Louisiana State University, Baton Rouge, Louisiana, 1984).

Given that the Landsat-4 MSS coherent noise can adversely affect analysis results, the noise should be characterized more precisely and a technique for filtering out the noise should be found. A characterization of the coherent noise and a description of a technique that filters out the noise while minimally affecting the image data itself follow.

The coherent noise pattern also appears in the original "integrating sphere" test data from the preflight Landsat-5 (Landsat-D′) MSS instrument. The noise characterization obtained suggested that certain filters be added to the Landsat-D′ MSS instrument. Subsequent integrating sphere test data show that the noise reduction filters did indeed eliminate a large part of the noise. Also, in-flight data from Landsat-5 confirm that the noise is substantially reduced. The Landsat-5 MSS results (preflight and in-flight) are presented following the discussion of Landsat-4 MSS results.

---

*Currently with Defense Mapping Agency HQ/STT, Washington, D.C. 20305.

†The ISOCLAS function was run with ISTOP = 12, CHNTHS = 1.0, DLMIN = 1.0, STDMAX = 1.5, and MAXCLS = 16, where ISTOP is the maximum number of iterations, CHNTHS is the threshold for cluster chaining, any two clusters whose means are closer than DLMIN are combined, any cluster whose standard deviation is greater than STDMAX, and whose number of points is greater than 2 (NMIN + 1) are split (where NMIN is the default 30 points), and MAXCLS is the maximum number of clusters.

ORIGINAL PAGE
COLOR PHOTOGRAPH

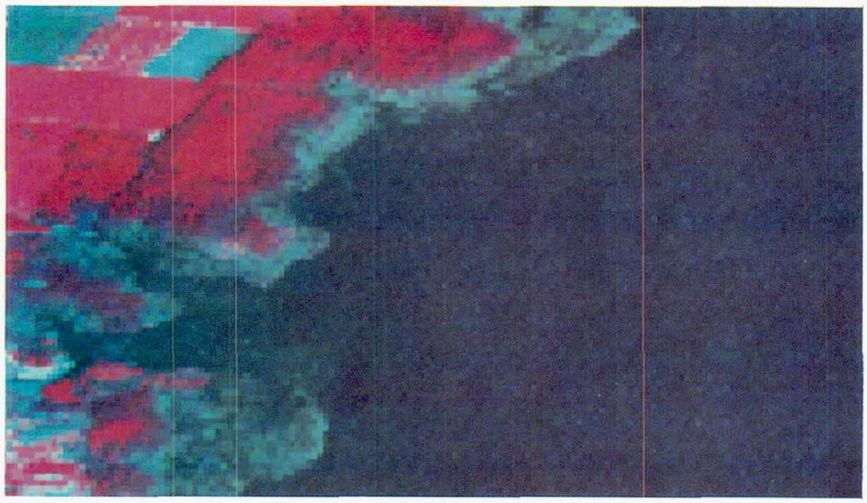

(a)

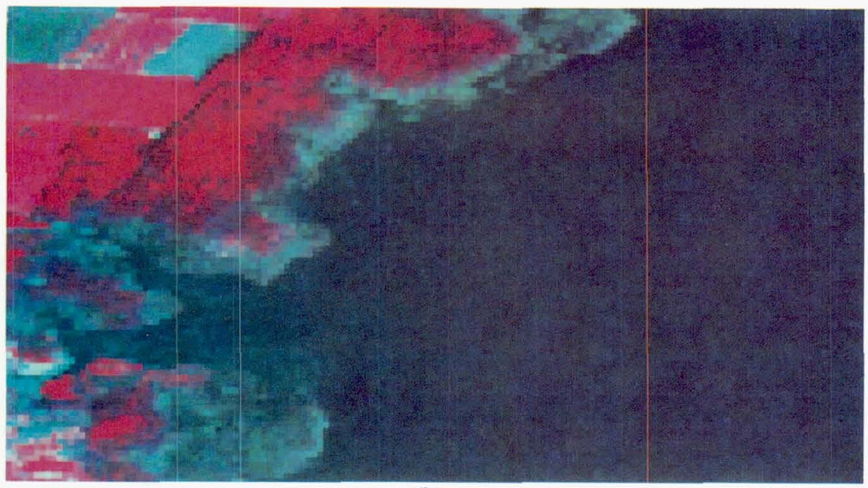

(b)

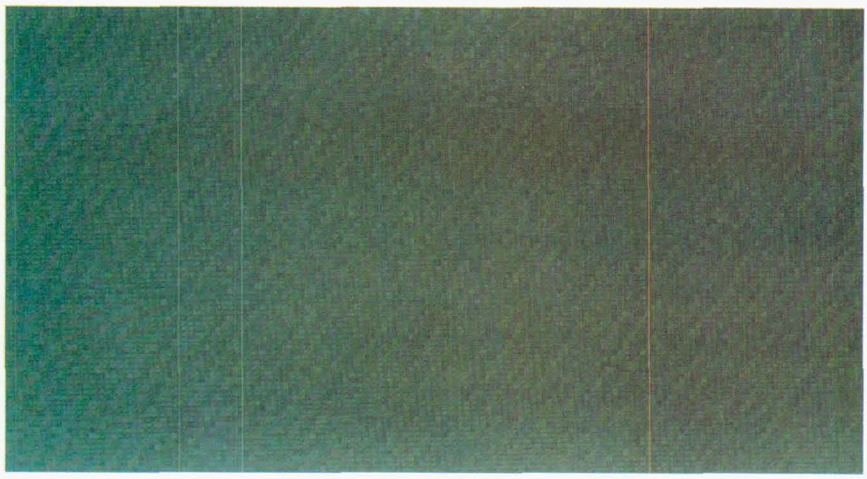

(c)

Figure 1. (a) Original, (b) filtered, and (c) difference image (plus bias) illustrating the Landsat-4 coherent noise problem. Shown is a 90-line by 157-column section of Landsat-4 MSS data (A-format CCT) over the coast of North Carolina obtained on September 24, 1982 (scene ID 84007015081, starting line 1801, starting column 2176).

ORIGINAL PAGE
COLOR PHOTOGRAPH

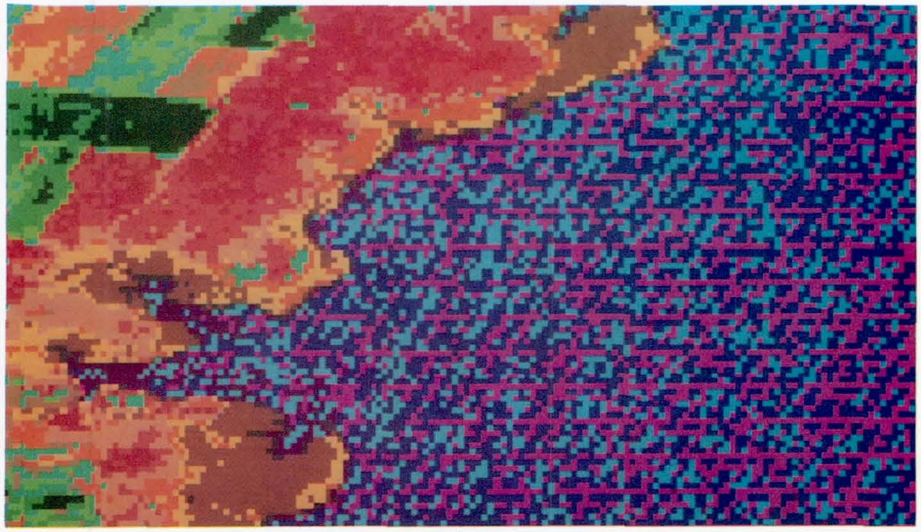

(a)

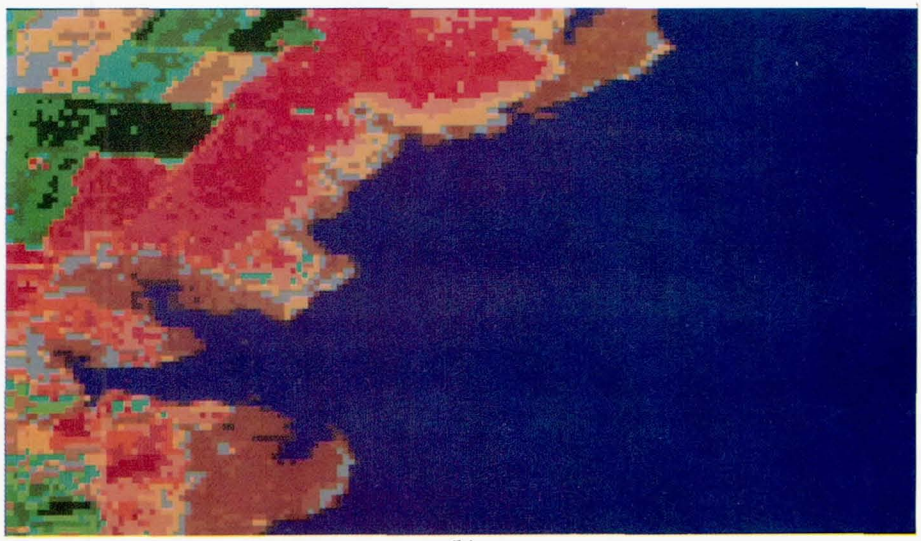

(b)

Figure 2. Cluster map of a 90-line, 157-column portion of Landsat-4 MSS data over the coast of North Carolina obtained on September 24, 1982 (scene ID 84007015081, starting line 1801, starting column 2176). (a) Original data. (b) Filtered data.

LANDSAT MSS SAMPLING SCHEMA

The noise characterization and filtering techniques investigated here are based on the manner in which the Landsat MSS systems gather image data. A simplified but fairly complete description of this process is given by Gordon (Reference 1). Further information particular to Landsat-4 and Landsat-5 can be found in Reference 2.

The Landsat MSS systems scan a 6-pixel swath each mirror forward scan. On an A-format Computer Compatible Tape (CCT), lines 1 through 6 are from the first forward mirror scan; lines 7 through 12 are from the second forward scan, and lines 6n-5 through 6n are from the nth forward scan. Since Landsat-4 and Landsat-5 are 4-band systems, 24 detectors are scanned in each forward scan.

Each detector is sampled in sequence. Let the four bands be designated by the numerals 1, 2, 3, and 4, and let the six rows in each scan be designated by the letters A, B, C, D, E, and F. With this coding, detector 1A corresponds to band 1, row 1; detector 2A corresponds to band 2, row 1; ...; and detector 4F corresponds to band 4, row 6. The sampling sequence is: 1A, 2A, 1B, 2B, 1C, 2C, 1D, 2D, 1E, 2E, 1F, 2F, 3A, 4A, 3B, 4B, 3C, 4C, 3D, 4D, 3E, 4E, 3F, 4F. After the 24 detectors are sampled, a blank is inserted (this blank was reserved for the far-infrared band on Landsat-3), and the sampling sequence is repeated. The time spacing between each individual sampling is 0.39832 microseconds, and the entire sequence (including the blank) is resampled every 25×0.39832 or 9.958 microseconds.

Because of the physical layout of the detectors for each band of the MSS, the ground pixel locations of the four bands are offset from each other. If the MSS is scanning from west to east, in each sampling sequence the ground pixel location of band 2 is actually 2 pixels west of the ground pixel location of band 1; band 3 is 4 pixels west of band 1, and band 4 is 6 pixels west of band 1. This band-to-band offset is corrected for in A-format CCTs by the addition of 6 fill pixels to the start of each band 1 line; 4 fill pixels to the start and 2 fill pixels to the end of each band 2 line; 2 fill pixels to the start and 4 fill pixels to the end of each band 3 line; and 6 fill pixels to the end of each band 4 line.

CHARACTERIZING THE NOISE

As mentioned previously, Landsat-4 MSS image data exhibit an irregular oscillating noise pattern roughly 3 to 4 pixels in period. A 3- to 4-pixel period corresponds to a noise frequency range of 25 to 34 kHz. This frequency range corresponds to no candidate noise sources in the MSS electronics that are known to the authors. Image domain data are effectively sampled with a 9.958 microsecond period, the period at which the entire 24-detector sequence is sampled. This sampling period corresponds to a sampling frequency of 100.42 kHz. With this sampling frequency any noise frequency at over 50.2 kHz will appear at an alias frequency, and its true frequency could not be determined with any certainty. An analysis of the MSS data carried out directly in the image domain has little hope of pinning down the source of the noise if the noise source has a frequency of over 50.2 kHz.

If the Landsat-4 MSS data were available in the original sampling sequence rather than image format, much higher frequency noise sources could be detected directly. As noted in the previous section, before the MSS data are put into image format, the data form a string of data points with a sampling period of 0.39832 microsecond, which corresponds to a sampling frequency of 2510 kHz. If the blank sample after each group of 24 detector samples is filled in by interpolation, the data could be analyzed as a string of samples taken at a sampling frequency 25 times that of the image domain sampling frequency. With a sampling frequency of 2510 kHz, the frequency of any noise source under 1255 kHz can be directly determined through the use of Fourier analysis. Since there are potential noise signals in the MSS electronics under 1255 kHz, there is some hope of pinning down the source of the noise when the data are analyzed in the original sampling sequence. In particular, one potential noise source is the power system with a nominal switching frequency of 110 kHz ± 5 kHz.

Landsat-4 or Landsat-5 MSS data are not available in the original sampling sequence. (Note: Landsat-4 and Landsat-5 are referred to as Landsat-D and Landsat-D′, respectively, prior to launch). Landsat MSS digital image data sets are normally available in two formats: A-format CCT and P-format CCT. P-format CCT data have undergone geometric resampling and are not appropriate for this study. The A-format CCT is the closest thing to the original sequence data that are readily available. Fortunately, the formating process that creates an A-format CCT from the original data stream is reversible. We call this reversal process "resequencing." (Besides formating into image format, A-format CCT data normally have undergone radiometric correction, though integrating sphere data taken prior to launch were not normally radiometrically corrected. However, the radiometric correction applied to A-format data is not enough to obscure the analysis of the coherent noise in Landsat-4

MSS because the coherent noise magnitude is large relative to the amount of radiometric correction. The analysis of the coherent noise in Landsat-5 MSS data may be obscured somewhat. For further discussion on this point see Reference 3.)

The first step in resequencing is to remove the fill pixels. Six pixels are deleted from the front of each line of band (i.e., column 7 of band 1 becomes column 1), 4 pixels are deleted from the front of each line of band 2; and 2 pixels are deleted from the front of each line of band 3. Next, the data from each 4-band, 6-line scan group are strung out according to the sampling sequence (see previous section) into one long data line. If an entire 2400-line, 3240-sample, 4-band MSS scene is resequenced from an A-format CCT, the resulting data file would consist of 400 (2400/6) lines with 80,849 (25*(3240-6)-1) samples in each line. As part of the resequencing process, a value is interpolated for the blank sample period, which occurs every 25n'th sample, n = 1,2...,3233. Thus, every 25n'th sample is the average of the 25n-1 sample and the 25n = 1 sample.

Once a portion of the MSS data is resequenced, it can be analyzed for possible noise frequencies. The most convenient way to do this is to take a one-dimensional Fourier transform of a piece of the data. Because the Fourier transform routine utilized can handle a maximum of 4096 samples, we analyzed 6-line, 170-sample sections of the 4-band MSS data, which when resequenced becomes 1 line by 4099 (25*(170-6)-1) samples. We take the Fourier transform of the first 4096 samples of this resequenced line of data.

One thing that is immediately noticed upon looking at a plot of the magnitude of the Fourier transform of the resequenced data is that the amplitude of the frequency component corresponding to the sampling frequency of 100.42 kHz (period of 9.958 microseconds), and its harmonics, completely swamp out everything else. This is due to the differences in response across the four bands. In order to minimize the amplitude of these particular frequency components, we must add (subtract) a bias to (from) each of the bands so that all four bands have the same mean value before the resequencing and Fourier transform are performed. When this is done, the 100.42 kHz frequency and its harmonics are suppressed on a magnitude plot of the Fourier transform, and the frequency components corresponding to the coherent noise stand out distinctly. Appendix A presents a detailed "cookbook" description of the Interactive Digital Image Manipulation System (IDIMS) facility at the NASA GSFC characterizing the coherent noise.

NOISE CHARACTERIZATION RESULTS

The noise characterization studies were carried out on the Landsat-D (prelaunch Landsat-4) and Landsat-D′ (prelaunch Landsat-5) MSS integrating sphere data, on three Landsat-4 MSS scenes, and one Landsat-5 MSS scene. The Landsat-D′ data included data from before and after installation of noise filters (see Table 1). Table 2 lists the specific 6 line by 170 sample sections of these data sets used in the analysis.

For each 6-line by 170-sample study site, separate biases were first added to (or subtracted from) each band to produce a mean value of 25 (after rounding) in each band. Each study site was then resequenced, and the magnitude of the Fourier transform of each resequenced data set was plotted. Several of these plots are included in Appendix B.

Table 1
Data Sets Analyzed

Description	Date	Scene ID
Integrating Sphere (Landsat-D)	Sept. 10, 1981	—
Integrating Sphere (Landsat-D′ no filters)	Sept. 16, 1982	—
Integrating Sphere (Landsat-D′ with filters)	Sept. 29, 1983	32005-13380
Louisiana, Lake Pontchartrain (Landsat-4)	Sept. 16, 1982	84006215591
North Carolina, Atlantic Ocean (Landsat-4)	Sept. 24, 1982	84007015081
Florida, Gulf of Mexico (Landsat-4)	March 31, 1984	84062415465
Florida, Gulf of Mexico (Landsat-5)	April 24, 1984	85005415465

Table 2
Noise Characterization Study Sites

Scene	Starting Line	Starting Pixel	Number of Lines	Number of Pixels
Integrating Sphere (Landsat-D)	13	2101	6	170
Integrating Sphere (Landsat-D)	1201	2101	6	170
Integrating Sphere (Landsat-D)	2383	2101	6	170
Integrating Sphere (Landsat-D′, no filters)	7	1621	6	170
Integrating Sphere (Landsat-D′, with filters)	7	1621	6	170
Louisiana (Landsat-4)	1423	1301	6	170
Louisiana (Landsat-4)	1261	1781	6	170
North Carolina (Landsat-4)	481	2001	6	170
Florida (Landsat-4)	433	131	6	170
Florida (Landsat-5)	433	11	6	170
Florida (Landsat-5)	433	341	6	170

Figure 3 shows the Fourier transform magnitude plot for the North Carolina study site. In the plot we notice two or three dozen peaks. Even though the study site is over a very radiometrically flat area (the Atlantic Ocean), not all of the peaks are due to coherent noise. Some peaks are due to the residual differences between band means that remain even after the means of each band are equalized. The residual differences remain because the discrete radiometric sampling does not allow exact equalization of means. Differences between detectors within each band may also contribute to these peaks. As mentioned earlier, these resequencing artifact peaks occur at a frequency of 100.42 kHz (period of 9.958 microseconds), and at the harmonics of this frequency. To identify these artifact peaks clearly on the Fourier transform magnitude plots, the magnitudes have been plotted versus image domain frequency (cycles/pixel). In this scale, the artifact peaks occur at integer values (1,2,3 ...). Note that 1 cycle/pixel in the image domain is equal to 1/25 cycle/sample in the resequenced sampling domain and to 100.42 kHz in the time domain.

The largest noise peak in the North Carolina study site Fourier transform plot (Figure 3) is at an image domain frequency of 2.28 cycles/pixel. This corresponds to a time domain frequency of approximately 229 kHz, very near the second harmonic of the power system switching frequency of 110 kHz ± 5 kHz.

The Fourier transform plots for each study site contain several peaks attributable to the coherent noise. These peaks are similar in amplitude and frequency across all study sites, and were constant in frequency across study sites within a particular data set. In each case the largest noise peak is very near the second harmonic of the power system switching frequency (see Table 3). This behavior is consistent with a hypothesis that the noise signal source is a slowly drifting oscillator, possibly in the dc to dc voltage converter or chopper voltage regulator.

The introduction noted that the coherent noise appears as an oscillating pattern approximately three to four pixels in period running roughly diagonal from NNE to SSW in the MSS imagery. Frequencies in the range of 226 to 230 kHz (2.25 to 2.29 cycles/pixel) will appear at an alias frequency of 25.1 to 29.1 kHz (0.25 to 0.29 cycles/pixel), or at a period of 3.4 to 4.0 pixels. This aliasing corresponds precisely to what is observed in the imagery.

Appendix C examines in more detail the coherent noise peaks seen in the Fourier transform magnitude plots, and offers possible explanations of the frequency relationships between the various peaks observed.

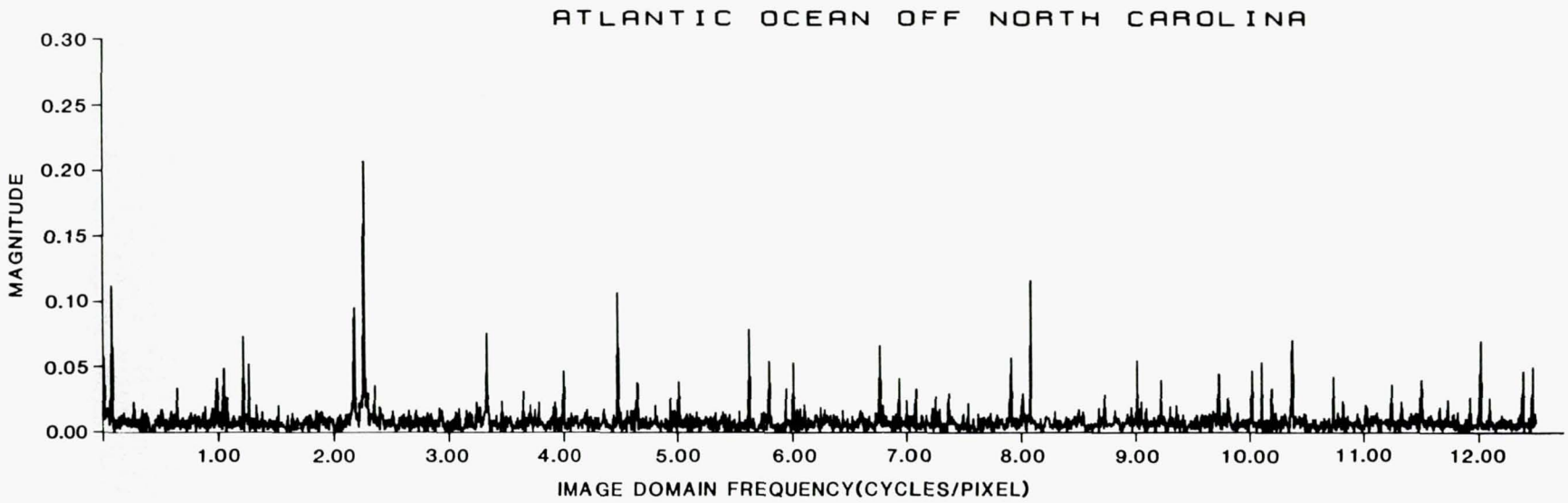

Figure 3. Fourier transform magnitude plot of 4096-sample resequenced sample study site. The site is of the Atlantic Ocean off the North Carolina coast. (Only the positive, nonzero frequency components are displayed; magnitude in counts.)

Table 3
Largest Coherent Noise Peaks
(Power system switching frequency is 110 kHz ±5 kHz)

Scene	Frequency (kHz)	Frequency/2 (kHz)
Integrating Sphere (Landsat-D)	228	114.0
Integrating Sphere (Landsat-D ′)	226	113.0
Louisiana (Landsat-4)	229	114.5
North Carolina (Landsat-4)	229	114.5
Florida (Landsat-4)	229	114.5
Florida (Landsat-5)	227	113.5

FILTERING LANDSAT-4 MSS COHERENT NOISE

A technique was devised through which the Landsat-4 MSS coherent noise can be removed with minimal effect on the ground image data. This technique was used to produce Figure 1b.

The first step is to characterize the coherent noise for the scene in question using the technique discussed in the Noise Characterization section. This gives us a list of frequency components corresponding to the coherent noise for that scene. The frequency component list for the example scene (Figure 1) is given in Table 4.

Table 4
Filter for Example Scene (Figure 1)

Noise Frequency Components		Blocking Filter Zeros
Image Domain Frequency (cycles/pixel)	Sample Domain Frequency (cycles/(4096 samples))	Sample Domain Frequency (cycles/pixel)
1.23	201	199-203
2.20 and 2.28	360 and 374	357-377
3.33	546	544-548
4.47	733	731-735
5.62	920	918-922
5.79	948	946-951
6.76	1107	1104-1109
6.93	1135	1133-1136
7.90	1294	1291-1296
8.07	1322	1320-1324
9.21	1509	1506-1511
10.35	1696	1692-1698
11.49	1882	1880-1885
12.37	2027	2025-2029
12.46	2041	2039-2043

Note: 25 samples = 1 image domain pixel.

Next a 0-1 blocking filter was designed based on the noise frequency component list. The blocking filter is set to all ones except in bands surrounding the noise frequency components where the filter is set to zero. The frequency components set to zero in our blocking filter for the example scene are also given in Table 4. The band of frequencies blocked around each noise frequency component is taken to be fairly broad (± 2 or 3 cycles/(4096 samples) from the peak) to allow for rounding the filter to reduce filtering artifacts.

A technique that is often used to round filters is to multiply the filter in the transform domain (here spatial domain) by an elliptical arc (Reference 4). Since the original 0 - 1 filter is so sharp, the rounding effect is increased using the square of an elliptical arc instead. The 4096 point squared elliptical arc is given by the formula:

$$E(x) = \begin{cases} 1.0 - \left(\dfrac{x-1}{2048}\right)^2 & \text{for } 1 <= x <= 2049 \\[2ex] 1.0 - \left(\dfrac{4097-X}{2048}\right)^2 & \text{for } 2049 < x <= 4096. \end{cases}$$

Next, we take an inverse Fourier transform of the blocking filter, multiply the result by the elliptical arc squared, and take a forward Fourier transform of the multiplication results. This gives the rounded blocking filter. Plots of one-half of the elliptical arc squared, the zero-one blocking filter, and the rounded blocking filter are given in Appendix D.

The next step is to filter the chosen section of data. In the example, a 90-line by 157-column section was filtered by starting with a 90-line by 170-column section. For each 6-line section (corresponding to the six MSS detectors per band), we resequence the data into the original sampling sequence (*without* adding biases to each band) giving 15 separate 1-line by 4099-column resequenced sections. Then take the 4096-point forward Fourier transform of each of these sections, multiply each by the rounded blocking filter, and take the inverse Fourier transforms. These filtered resequenced sections are then "inverse" resequenced back into image format. (One column of data is effectively lost by taking a Fourier transform of 4096 points rather than 4099 points, and another 12 columns are lost in the "inverse" resequencing process. Thus a 90-line by 157-column filtered image is produced from an original 90-line by 170-column A-format CCT tape image.)

A detailed "cookbook" description of the filtering performance using the IDIMS facility at the NASA GSFC is presented in Appendix A.

RETROFIT OF LANDSAT-D' TO REMOVE COHERENT NOISE

After the initial study of the Landsat-4 and D′ MSS coherent noise, General Electric (GE) installed electronic (RC) low-pass filters at the output of each detector. GE integrating sphere data from the retrofitted Landsat-D′ MSS instrument (scene 32005-13380, dated Sept. 29, 1983) were received. By comparing these data with the original integrated sphere data, the RC filters were found to reduce the coherent noise level by nearly 25 percent. Most noise peaks were reduced in magnitude to the magnitude levels of the random noise components. Only the peaks at 0.19, 2.26, 2.45, and 4.70 cycles/pixel remained, and these were reduced in magnitude by factors of approximately 0.25, 0.50, 0.28, and 0.22. (These peaks were shifted by oscillator drift to 0.20, 2.25, 2.45, and 4.71 cycles/pixel in the RC filtered data. See Appendix B.) This includes the coherent noise peak at the image domain frequency of 0.190 cycles/pixel (time domain frequency of 19.00 kHz), which is below the roll-off of RC filter. (The RC filter is designed to block only image domain frequencies above 1 cycle/pixel.) The harmonic theory advanced in Appendix C quite easily explains the absence of this peak since it postulates that the peak is actually an alias from 24.81 cycles/pixel.

Figure 4 displays magnitude plots of the Fourier transform of resequenced portions of mean equalized Landsat-D′ integrating sphere data before and after retrofit. Note the lack of coherent noise peaks in the plot for the retrofitted case. A more detailed look at the data can be found in Appendix B.

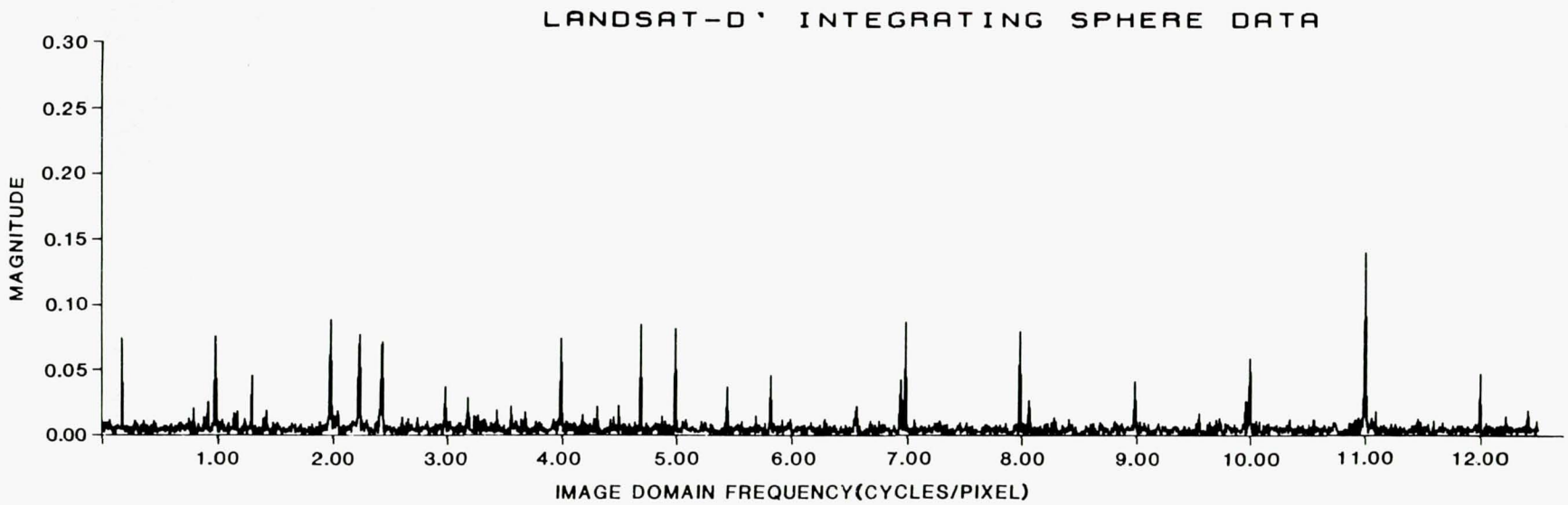

Figure 4a. Fourier transform magnitude plots of 4096-sample resequenced sample of integrating sphere data from the original. (Only the positive, nonzero frequency components are displayed; magnitude in counts.)

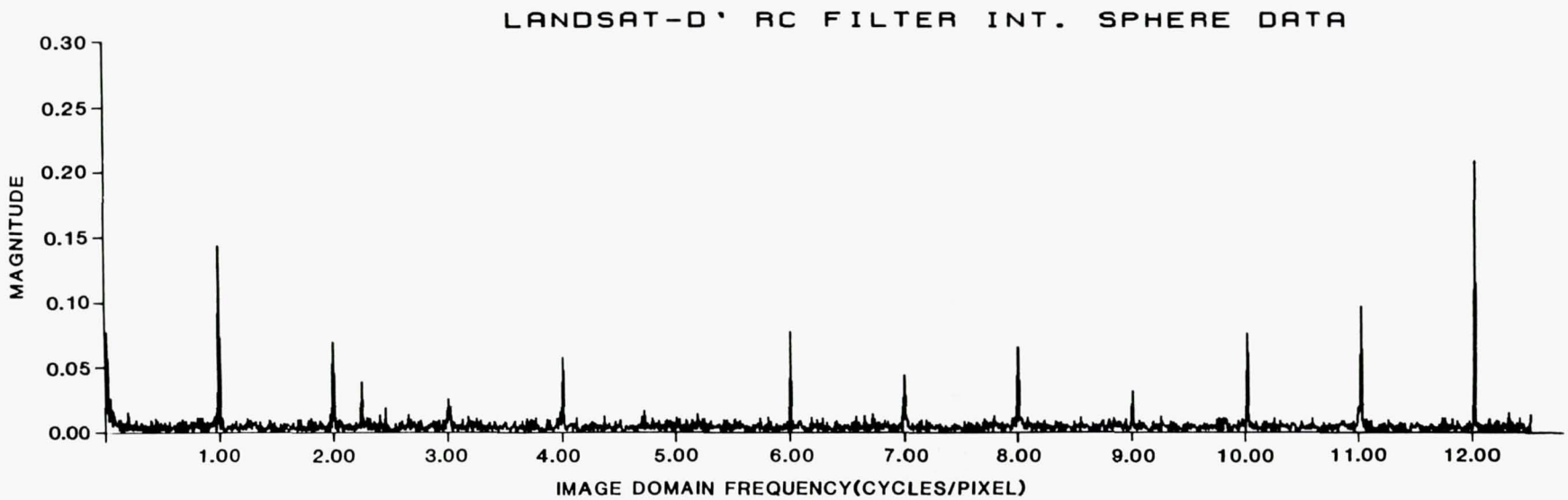

Figure 4b. Fourier transform magnitude plots of a 4096-sample resequenced sample of integrating sphere data from the retrofitted Landsat-D′ MSS instrument. (Only the positive, nonzero frequency components are displayed; magnitude in counts.)

CONCLUDING REMARKS

Both a technique for characterizing the coherent noise found in Landsat-4 and Landsat-5 MSS data and a companion technique for filtering out the coherent noise were described. The techniques were demonstrated on Landsat-4 and Landsat-5 MSS data sets (both preflight and in-flight), and explanations of the noise pattern were suggested in Appendix C. A cookbook procedure for characterizing and filtering the coherent noise using special NASA/Goddard IDIMS functions was included in Appendix A. Also described were analysis results from the retrofitted Landsat-5 MSS sensor, which show that the coherent noise has been substantially reduced.

The filtering technique presented in this report can be used to filter out the coherent noise present in the Landsat-4 MSS data already collected. Because the cleanup of Landsat-4 MSS data would be fairly expensive in terms of computer resources, it is expected that it would only be done for selected high-demand scenes. Assuming the RC filters installed by GE on the Landsat-D′ MSS continue to perform as well as they did on the test data set analyzed, it is expected that there will be no need to perform any ground-based filtering on data produced by Landsat-5.

REFERENCES

1. Gordon, Frederick, Jr., "The Time-Space Relationships of the Data Points (Pixels) of the Thematic Mapper and Multi-Scanner or 'The Myth of Simultaneity,' " *NASA Technical Paper 1715,* July 1980.

2. "Landsat-4 To Ground Station Interface Description," *NASA Technical Paper 436-D-400,* Revision 8, June 1984.

3. Tilton, James C., Brian L. Markham, and William L. Alford, "Landsat-4 and Landsat-5 MSS Coherent Noise: Characterization and Removal," *Photogrammetric Engineering and Remote Sensing,* Vol LI, No. 9, September 1985.

4. Frieden, B. Roy, "Image Enhancement and Restoration," in *Topics in Applied Physics, Volume 6: Picture Processing and Digital Filtering,* edited by T. S. Huang, Springer-Verlag, p. 196.

APPENDIX A

CHARACTERIZATION AND REMOVAL OF COHERENT NOISE FROM LANDSAT MSS IMAGERY DATA USING THE IDIMS FACILITY AT THE NASA GODDARD SPACE FLIGHT CENTER

In this Appendix we describe step-by-step how to characterize the Landsat MSS coherent noise and filter it out using the IDIMS facility at the NASA Goddard Space Flight Center. We assume that the reader has a basic familiarity with the IDIMS system: how to log on, enter into IDIMS, and use standard IDIMS functions. Included in this description is an example taken from our analysis and filtering of a portion of the North Carolina data set (see Figure 1 and Table 1 in the main body of this report).

(Note: The Landsat MSS data used throughout this analysis must be from an *A-format CCT.*)

Characterizing the Noise:

The first step in characterizing the coherent noise is to find a relatively uniform 6-line by 170-sample portion of data to analyze. The first line of this portion of data must be from the first sensor in the group of six MSS sensors (per band). This will be the case if the first line number satisfies (1 + 6x) where x is zero or a positive integer. A good way to find an appropriate section of data is to display the scene on the COMTAL or DEANZA display and use the track ball to identify the image coordinates of the portion of data.

Once the image data section is identified, the band means must be equalized. To do this run the IDIMS function PICSTAT on the 6-line by 170-sample portion of data you are analyzing, and note the band-by-band mean values. In the North Carolina example we have:

```
NC81.TEST4>PICSTAT
PLEASE SUPPLY PARAMETER VALUES FOR FUNCTION PICSTAT
DEVICE CHAR STRING (DEFAULT=TERM):
```

	MINIMUM			MAXIMUM				
DSRN	LINE	SAMP	VALUE	LINE	SAMP	VALUE	MEAN	VARIANCE
1	1	146	1.2000E+01	3	11	1.8000E+01	1.5018E+01	1.0801E+00
1	3	121	3.000E+00	4	8	1.1000E+01	7.7216E+00	8.8718E-01
1	1	56	1.000E+00	1	4	7.0000E+00	4.0431E+00	1.2256E+00
1	1	36	0.000E+00	1	2	2.0000E+00	9.7647E-01	1.2494E-01

```
End Function—PICSTAT
```

We add 9.982 to band 1, 17.2784 to band 2, 20.9569 to band 3, and 24.02353 to band 4 to make the mean of each band equal to 25.000. We accomplish this by using the IDIMS function LINEAR as follows:

```
NC81.TEST4[1]>LINEAR>B1
PLEASE SUPPLY PARAMETER VALUES FOR FUNCTION LINEAR
A    SIMPLE REAL (DEFAULT=.100000E+01):
B    SIMPLE REAL (DEFAULT=.000000E+00): 9.982
End Function—LINEAR
NC81.TEST4[2]>LINEAR>B2
PLEASE SUPPLY PARAMETER VALUES FOR FUNCTION LINEAR
A    SIMPLE REAL (DEFAULT=.100000E+01): 1
B    SIMPLE REAL (DEFAULT=.000000E+00): 17.2784
End Function—LINEAR
```

```
NC81.TEST4[3] > LINEAR > B3
PLEASE SUPPLY PARAMETER VALUES FOR FUNCTION LINEAR
A     SIMPLE REAL (DEFAULT = .100000E + 01):
B     SIMPLE REAL (DEFAULT = .000000E + 00): 20.9569
End Function—LINEAR
NC81.TEST4[4] > LINEAR > B4
PLEASE SUPPLY PARAMETER VALUES FOR FUNCTION LINEAR
A     SIMPLE REAL (DEFAULT = .100000E + 01):
B     SIMPLE REAL (DEFAULT = .000000E + 00): 24.02353
End Function—LINEAR
```

(Note: We could have subtracted 15.018 from band 1, 7.7216 from band 2, 4.0431 from band 3, and 0.97647 from band 4 to produce a zero mean (real) image.)

We now have four separate single-band images: B1, B2, B3, and B4. We can combine them into a 4-band multispectral image using the IDIMS function UNITE (we disable the ASAP (array processor) here because it often malfunctions on images with very few lines or columns):

```
> SET (ASAP = DISABLE)
B1  B2  B3  B4 > UNITE > N. CAR MEANEQ
PLEASE SUPPLY PARAMETER VALUES FOR FUNCTION UNITE
SPECTYPE CHAR STRING (DEFAULT = BB):
End Function—UNITE
```

To check our results we can rerun PICSTAT on our mean equalized test image:

```
N.CAR.MEANEQ > PICSTAT
PLEASE SUPPLY PARAMETER VALUES FOR FUNCTION PICSTAT
DEVICE CHAR STRING (DEFAULT = TERM):
```

	MINIMUM			MAXIMUM				
DSRN	LINE	SAMP	VALUE	LINE	SAMP	VALUE	MEAN	VARIANCE
1	1	146	2.1982E + 01	3	11	2.7982E + 01	2.5000E + 01	1.0801E + 00
1	3	121	2.0278E + 01	4	8	2.8278E + 01	2.5000E + 01	8.8721E.01
1	1	56	2.1957E + 01	1	4	2.7957E + 01	2.5000E + 01	1.2257E + 00
1	1	36	2.4024E + 01	1	2	2.6024E + 01	2.5000E + 01	1.2502E-01

```
End Function—PICSTAT
```

Our test image was indeed properly mean equalized since each band has a mean of 25.000. Now we can use the special Goddard IDIMS function RESEQ to put the data into the original sampling order:

```
N.CAR.MEANEQ > RESEQ > N.CAR.RESEQ
PLEASE SUPPLY PARAMETER VALUES FOR FUNCTION RESEQ
TYPE  CHAR  STRING  (DEFAULT = FORWARD):
End Function—RESEQ
```

We now take the first 4096 samples from the one line, 4100 sample image produced by RESEQ, and calculate the forward Fourier transform using the special Goddard IDIMS function CFFT1G, and take the magnitude of the result using the IDIMS function MAG. We then can plot the magnitude of the Fourier transform using the IDIMS function PLOT, as in the following example:

```
N.CAR.RESEQ (1 1 1 4096) > CFFT1G MAG > N.CAR.FFTMAG
  DIRECT FOURIER TRANSFORM
End Function—CFFT1G
End Function—MAG
```

```
N.CAR.FFTMAG (1  2  1  2050)>COPY PLOT
HIGH IMPACT PROGRAM - DO NOT RUN ON LARGE IMAGES DURING PRIME TIME
End Function—COPY
CONTROL-Y AVAILABLE
PLEASE SUPPLY PARAMETER VALUES FOR FUNCTION PLOT
SUBSAM SIMPLE INTEGER (DEFAULT=1):
DEVICE CHAR STRING (DEFAULT=LP):
CONTROL-Y DISABLED
End Function—PLOT
```

We plotted samples 2 through 2051 in our example in order to prevent the dominant zero frequency component from swamping out all other frequency components in the plot, and included the IDIMS function COPY in the command line to shift the image by one pixel giving us an X-axis running from 1 to 2050. Plotted in this way, the X-axis values are equal to sample domain frequencies (cycles/(4096 samples)), and the Nyquist frequency is plotted at 2048 cycles/(4096 samples) or 0.5 cycles/sample. We plotted only 2050 points because the points on the X-axis from 2049 to 4096 are a mirror image of the points on the X-axis from 1 through 2047.

The plot using the foregoing process will be approximately 33 pages long. The Fourier transform magnitude plots included in Appendix B are compressed versions of plots generated in this way.

(Note: If we had mean equalized to a zero mean (forcing a zero value for the zero frequency term), we still would want to use COPY to shift the axis so that the X-axis values are equal to cycles per 4096 samples.)

(Note: Since the test data are discrete (byte) data, the mean equalization does not have to be exact. We could have added 10.0 to band 1, 17.0 to band 2, 21.0 to band 3, and 24.0 to band 4, and would have virtually the same Fourier transform magnitude plot as the end result.)

Filtering Out the Coherent Noise:

We now describe the process of filtering the coherent noise out of an arbitrary 90 line by 157 column section of Landsat-4 or D′ data (the first line number of the section must again satisfy $(1+6x)$ where x is zero or a positive integer).

We first need to create a 0 - 1 blocking filter with 0's at bands of frequencies corresponding to coherent noise peaks on the Fourier transform magnitude plot created as in the Characterizing the Noise section. The zeros should cover a band of frequency components surrounding the noise peaks (e.g., ± 2 or more cycles/sample). The set of zeros used in the North Carolina example is given in Table 4.

(Note: Referring to Table 4, we could have added a band of zeros around 14 cycles/(4096 samples), but opted not to out of fear of filtering out ground signal information in that frequency band. Also, the filter may have worked as well if we didn't include bands of zeros at the weaker noise peaks such as at 1135, 1509, 1882, 2028 and 2041 cycles/(4096 samples).

We can use the IDIMS functions CONSTANT, MOSAIC, and MIRROR to create a specific 0 - 1 blocking filter. It is most convenient to set up an IDIMS command file to perform the operations involved. We can best describe how this is done by referring to the command file we used to create the 0 - 1 blocking filter for the North Carolina example:

```
COMMENT: COMMAND FILE FOR CREATING THE
COMMENT: 0 - 1 BLOCKING FILTER FOR THE
COMMENT: NORTH CAROLINA STUDY AREA
COMMENT:
>SET(ASAP=DISABLE PROMPT=NOOPT)
>CONSTANT (DATATYPE=4 NL=1 NS=200 GRAYLEVL=1.0)>ONES
>CONSTANT (DATATYPE=4 NL=1 NS=25 GRAYLEVL=0.0)>ZEROS
ONES (1 1 1 199 ZEROS (1 1 1 5) ONES (1 1 1 153) ZEROS (1 1 1 21) +
ONES (1 1 1 166) ZEROS (1 1 1 5) ONES (1 1 1 182) ZEROS (1 1 1 5) +
```

```
ONES (1 1 1 182) ZEROS (1 1 1 5) ONES (1 1 1 23) ZEROS (1 1 1 6) +
ONES (1 1 1 152) ZEROS (1 1 1 6) ONES (1 1 1 23) ZEROS (1 1 1 4) +
ONES (1 1 1 154) ZEROS (1 1 1 6) ONES (1 1 1 23) ZEROS (1 1 1 5) +
ONES (1 1 1 181) ZEROS (1 1 1 6) ONES (1 1 1 180) ZEROS (1 1 1 7) +
ONES (1 1 1 181) ZEROS (1 1 1 6) ONES (1 1 1 139) ZEROS (1 1 1 5) +
ONES (1 1 1 9) ZEROS (1 1 1 5) ONES (1 1 1 5) +
>MOSAIC(PINLINE=31)>T1
>LISTCAT
T1(1 2 1 2047)>MIRROR>T2
T1 T2>MOSAIC (PINLINE=2)>N.CAR.01FILT
>SET(ASAP=ENABLE PROMPT=OPT)
T1 T2 ONES ZEROS>DELETE
```

The 0 - 1 blocking filter could be used as is, but the abruptness of the filter would cause filtering artifacts. This ''harsh'' 0 - 1 blocking filter can be ''softened'' a bit by multiplying the inverse Fourier transform of the filter by an elliptical arc (squared) and taking the Fourier transform of the product. Using the resulting ''rounded'' blocking filter produces a filter product virtually devoid of filtering artifacts.

An elliptical arc (squared) can be created by using the IDIMS SHADE, POWER, LINEAR, MIRROR, and CONVERT functions, viz.:

```
>SHADE POWER LINEAR > POS. ELLP
PLEASE SUPPLY PARAMETER VALUES FOR FUNCTION SHADE
DATATYPE SIMPLE INTEGER: 4
LORT SIMPLE REAL (DEFAULT= .000000E+00):
HORV CHAR STRING (DEFAULT=H):
NL SIMPLE INTEGER: 1
NS SIMPLE INTEGER: 2049
RORB SIMPLE REAL (DEFAULT= .255000E+03): 1.0
NLEVL SIMPLE INTEGER (DEFAULT=2049):
BANDS SIMPLE INTEGER (DEFAULT=1):
SPECTYPE CHAR STRING (DEFAULT=BB):
End Function—SHADE
PLEASE SUPPLY PARAMETER VALUES FOR FUNCTION POWER
EXP SIMPLE REAL (DEFAULT= .200000E+01):
End Function—POWER
PLEASE SUPPLY PARAMETER VALUES FOR FUNCTION LINEAR
A  SIMPLE REAL (DEFAULT= .100000E+01): -1.0
B  SIMPLE REAL (DEFAULT= .000000E+00): 1.0
End Function—LINEAR
POS. ELLP (1 2 1 2047) > MIRROR > NEG. ELLP
HIGH IMPACT PROGRAM — DO NOT RUN ON LARGE IMAGES DURING PRIME TIME
End Function—MIRROR
POS. ELLP NEG.ELLP > MOSAIC(PINLINE=2)>ELLP
End Function—MOSAIC
```

The "rounded" blocking filter for the North Carolina example is then created as follows:

```
ELLP > CONVERT (OUTYPE=COMPLEX) > ELLP.COMP
PLEASE SUPPLY PARAMETER VALUES FOR FUNCTION CONVERT
SPECTYPE CHAR STRING (DEFAULT=SAME):
End Function—CONVERT
```

```
N.CAR.01FILT > CONVERT(OUTYPE=COMPLEX) CIFT1G >N. CAR.01FILT.SPA
PLEASE SUPPLY PARAMETER VALUES FOR FUNCTION CONVERT
SPECTYPE CHAR STRING (DEFAULT=SAME):
End Function—CONVERT
  INVERSE FOURIER TRANSFORM
End Function—CIFT1G
N.CAR.01FILT.SPA ELLP.COMP > MULTIPLY CFFT1G > N.CAR.01FILT.ELLP
End Function—MULTIPLY
  DIRECT FOURIER TRANSFORM
End Function—CFFT1G
```

Now that we have our filter, we can remove the coherent noise from selected 90-line by 157-column portions of the data. Again, the first line number of the data section must satisfy (1 + 6x) where x is zero or a positive number. It is most convenient to use a command file to do the filtering operation (or set up a stream job). The command file we used in the North Carolina example follows:

```
COMMENT: COMMAND FILE FOR FILTERING THE
COMMENT: PERIODIC NOISE IN LANDSAT-4 MSS DATA
COMMENT:
COMMENT: SET UP THE FOLLOWING DEFINITIONS
COMMENT: INIM: YOUR INPUT IMAGE
COMMENT: FILTER: THE FILTER IMAGE (COMPLEX DATA TYPE)
COMMENT: OUTIM: THE FINAL OUTPUT IMAGE
COMMENT: SL= \ THE STARTING LINE OF THE IMAGE \
COMMENT: SS= \ THE STARTING SAMPLE OF THE IMAGE \
COMMENT:
INIM: N.CAR.ORIG
SS= \ 1 \
SL= \ 1 \
FILTER: N.CAR.01FILT.ELLP
OUTIM:N.CAR.FILTERED
>SET(PROMPT=NOOPT ASAP=DISABLE)
DO I=1 UNTIL 15
SLT= \ $SL+($I-1)*6 \
INIM ($SLT $SS 6 170)>RESEQ CONVERT (OUTYPE=COMPLEX)>
*(1 1 1 4096)>CFFT1G>
*FILTER>MULTIPLY CIFT1G RE RESEQ (TYPE=INVERSE)+
LINEAR (A=1.0 B=.5) +
CONVERT (OUTYPE=BYTE)>T.$I
NEXT I
T.1 T.2 T.3 T.4 T.5 T.6 T.7 T.8 T.9 T.10 +
T.11 T.12 T.13 T.14 T.15 +
>MOSAIC (PINLINE=1)>OUTIM
T.1 T.2 T.3 T.4 T.5 T.6 T.7 T.8 T.9 T.10 +
T.11 T.12 T.13 T.14 T.15 +
>DELETE
>SET(PROMPT=OPT ASAP=ENABLE)
INIM:
OUTIM:
FILTER:
```

The input image must be a 90-line by 170-column section of data centered on the 90-line by 157-column section to be filtered. The command file above produces a 90-line by 170-column image product as output, but the first 6 and last 7 columns are garbage, giving a 90-line by 157-column filtered section.

APPENDIX B

FOURIER MAGNITUDE PLOTS OF RESEQUENCED DATA FROM THE LANDSAT MSS COHERENT NOISE CHARACTERIZATION STUDY

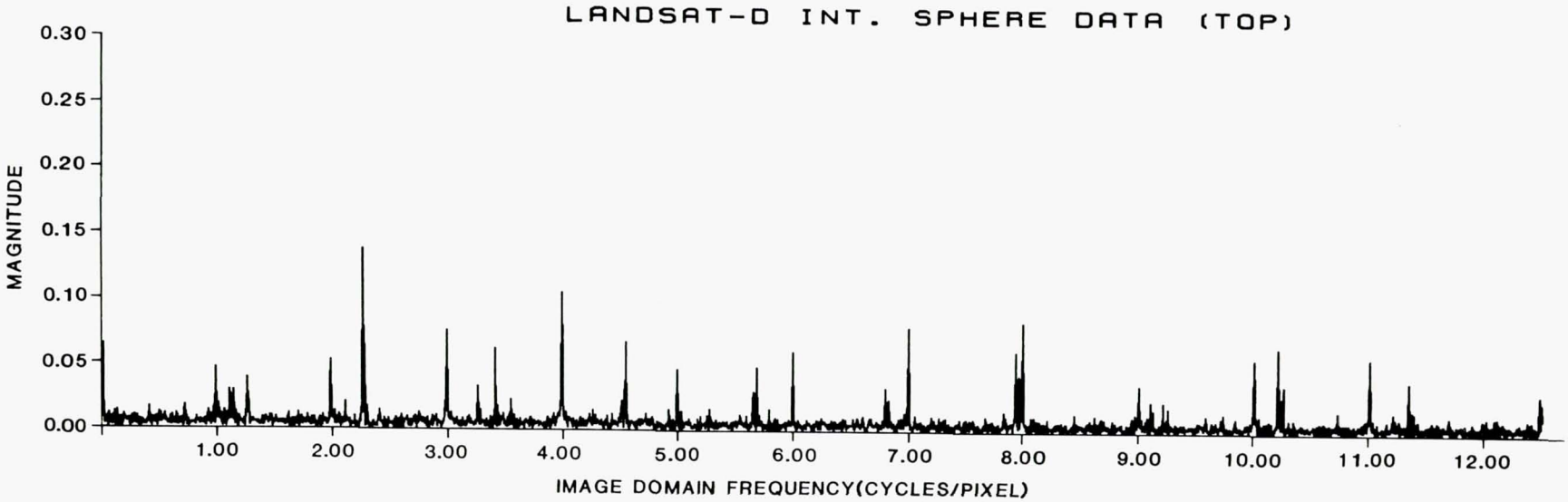

Figure B-1. Fourier transform magnitude plot of a 4096-sample resequenced section of Landsat-D MSS integrating sphere data. Data are a 6-line by 170-pixel section starting at line 13 and pixel 2101 from an integrating sphere data set obtained on September 10, 1981. Only the positive, nonnegative frequency components are displayed; magnitude is in counts.

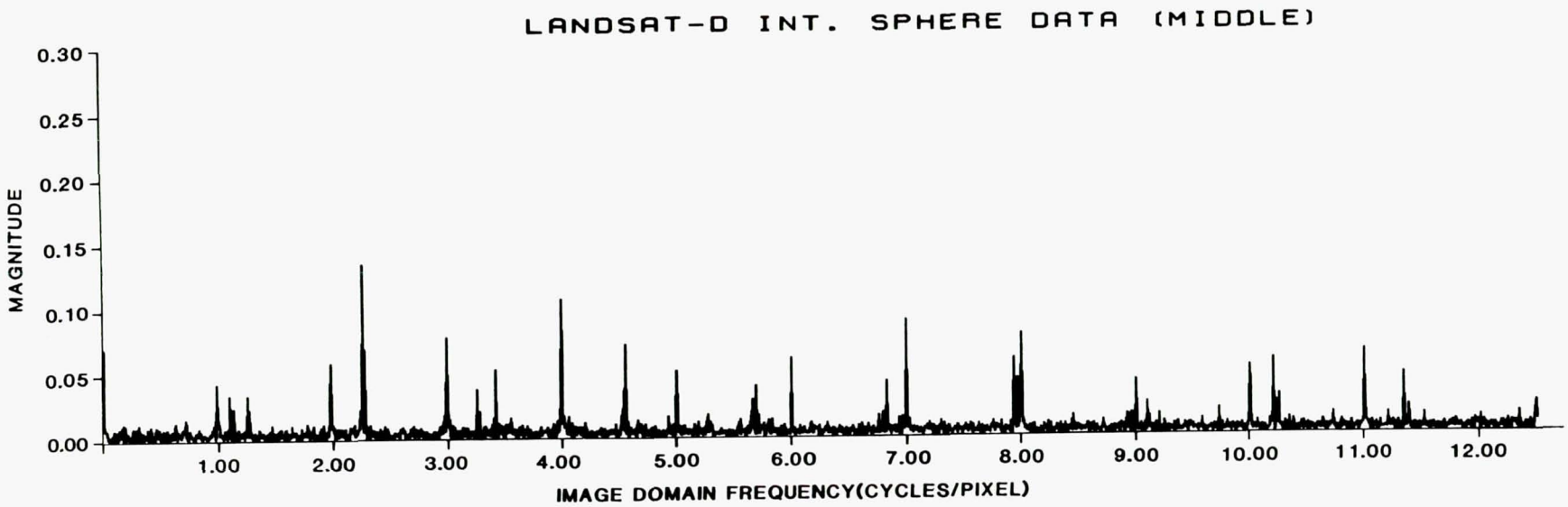

Figure B-2. Fourier transform magnitude plot of a 4096-sample resequenced section of Landsat-D MSS integrating sphere data. Data are a 6-line by 170-pixel section starting at line 1201 and pixel 2101 from an integrating sphere data set obtained on September 10, 1981. Only the positive, nonnegative frequency components are displayed; magnitude is in counts.

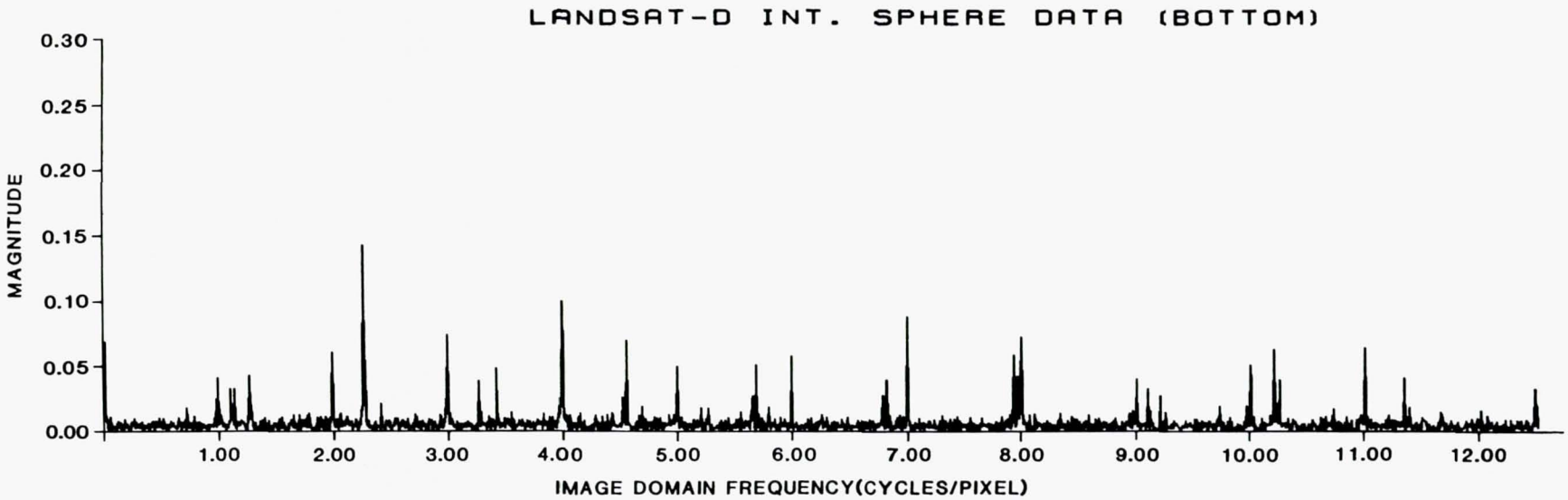

Figure B-3. Fourier transform magnitude plot of a 4096-sample resequenced section of Landsat-D MSS integrating sphere data. Data are a 6-line by 170-pixel section starting at line 2383 and pixel 2101 from an integrating sphere data set obtained on September 10, 1981. Only the positive, nonnegative frequency components are displayed; magnitude is in counts.

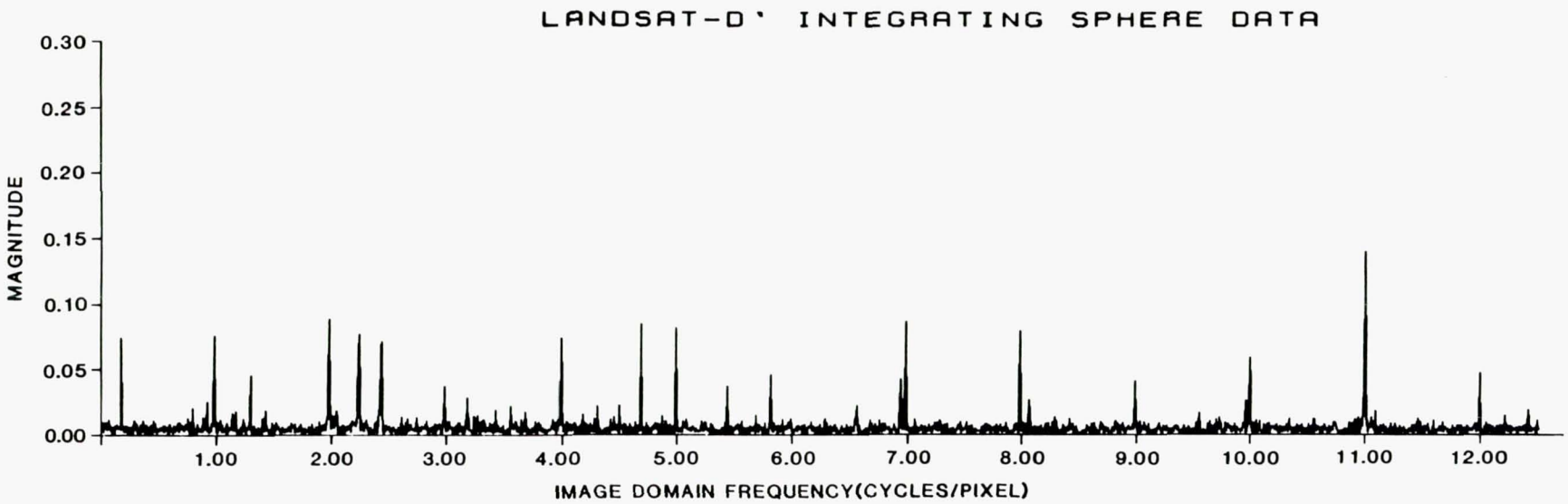

Figure B-4. Fourier transform magnitude plot of a 4096-sample resequenced section of Landsat-D' MSS integrating sphere data. Data are a 6-line by 170-pixel section starting at line 7 and pixel 1621 from an integrating sphere data set obtained on September 16, 1982. Only the positive, nonnegative frequency components are displayed; magnitude is in counts.

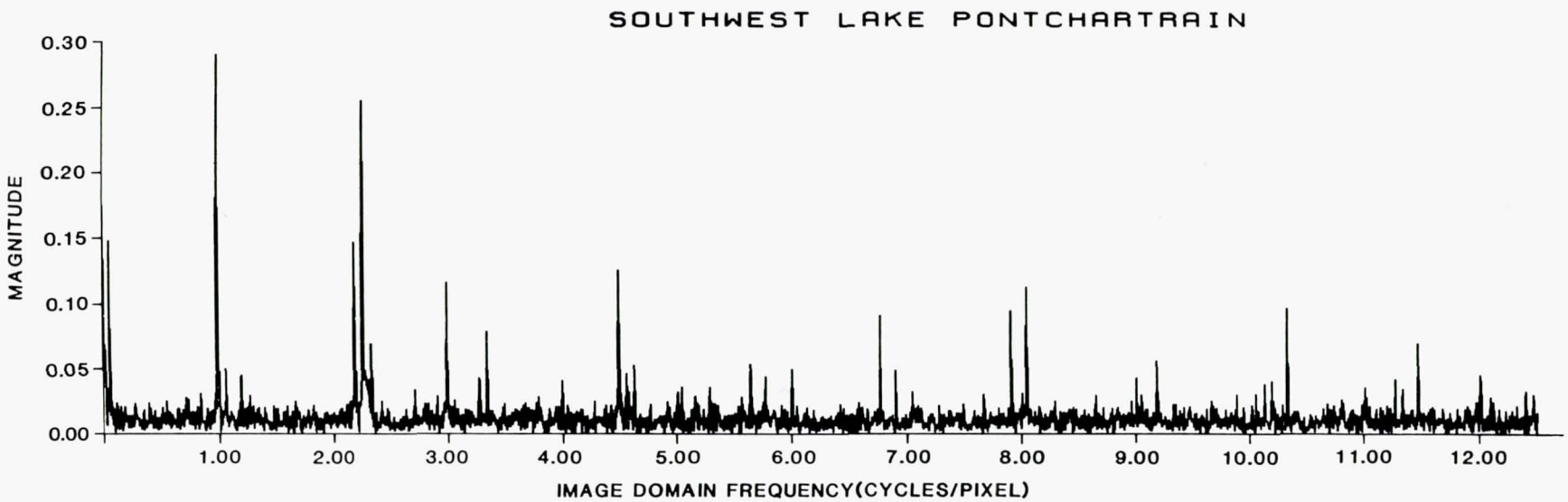

Figure B-5. Fourier transform magnitude plot of a 4096-sample resequenced section of Landsat-4 MSS imagery over Louisiana. Data are a 6-line by 170-pixel section starting at line 1423 and pixel 1301 from scene ID#84006215591 obtained on September 16, 1982. Only the positive, nonnegative frequency components are displayed; magnitude is in counts.

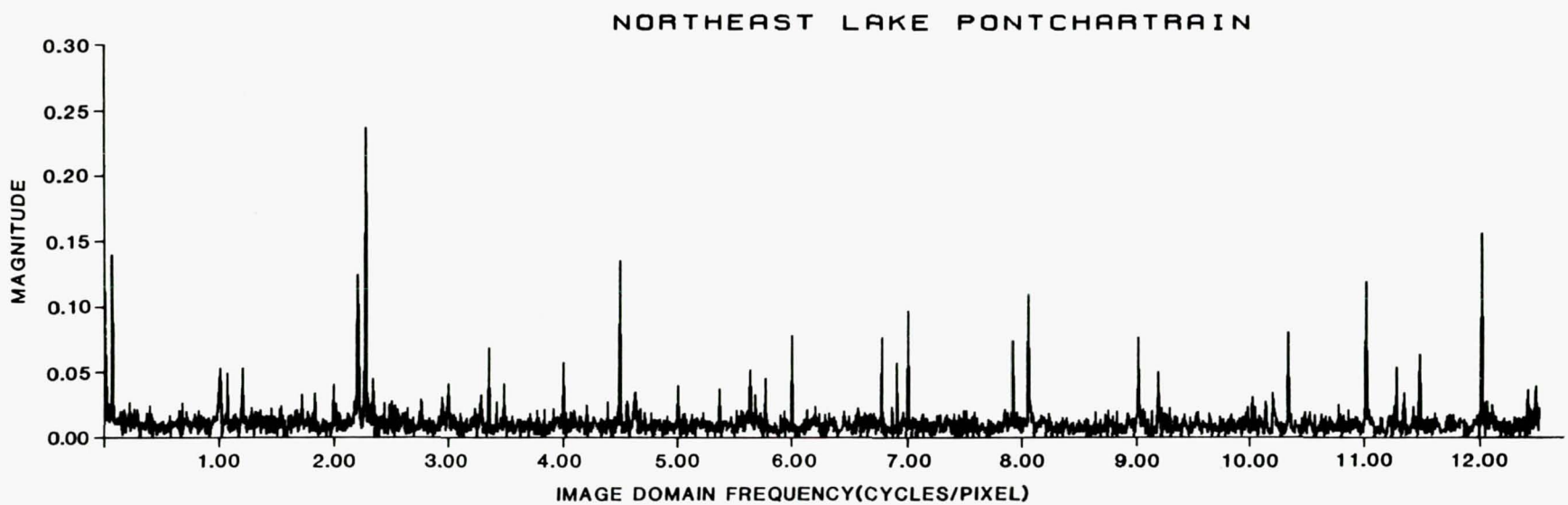

Figure B-6. Fourier transform magnitude plot of a 4096-sample resequenced section of Landsat-4 MSS imagery over Louisiana. Data are a 6-line by 170-pixel section starting at line 1261 and pixel 1781 from scene ID#84006215591 obtained on September 16, 1982. Only the positive, nonnegative frequency components are displayed; magnitude is in counts.

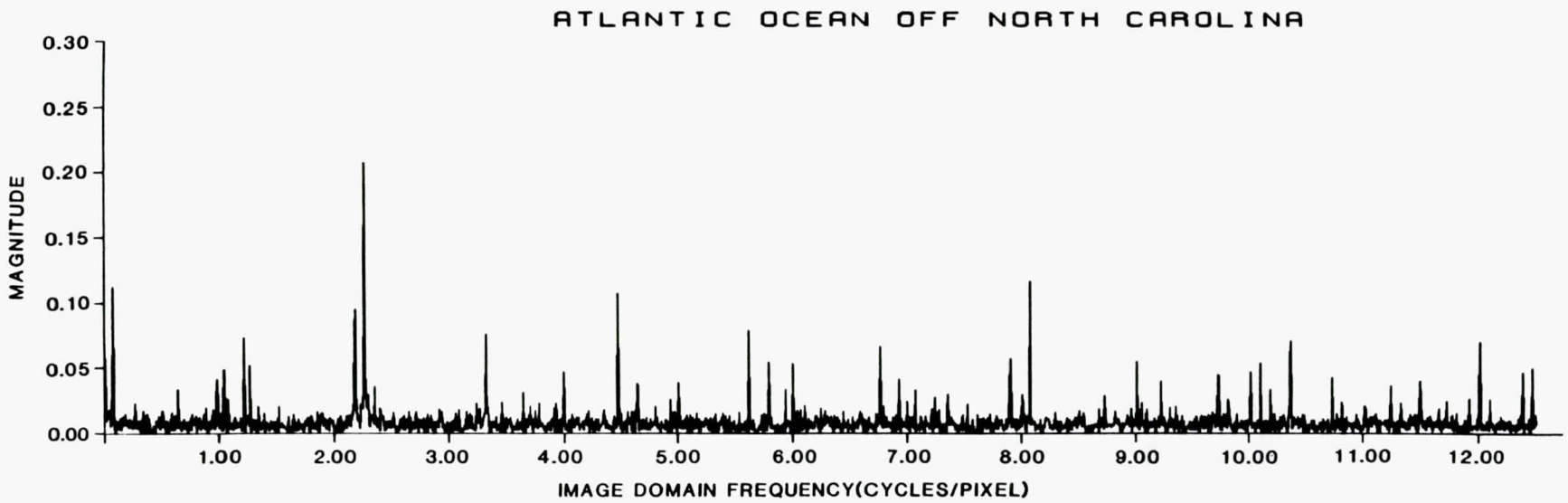

Figure B-7. Fourier transform magnitude plot of a 4096-sample resequenced section of Landsat-4 MSS imagery over North Carolina. Data are a 6-line by 170-pixel section starting at line 481 and pixel 2001 from scene ID#84007015081 obtained on September 24, 1982. Only the positive, nonnegative frequency components are displayed; magnitude is in counts.

APPENDIX C

DETAILED LOOK AT THE RESULTS FROM THE LANDSAT MSS COHERENT NOISE STUDY

Tables C-1 through C-6 list the coherent noise peaks observed in the various Landsat MSS data sets analyzed. (See Table 2 in the main body of this report for a description of the sections of data analyzed.) The tables give the spatial frequency of the noise peaks in terms of cycles per 4096 samples (the natural axis of the Fourier transform plot) and in terms of cycles per pixel. (Because of the resequencing operation, 1 image domain pixel corresponds to 25 resequenced domain samples.) Also given is the image domain period of each noise peak as it would appear in the image (i.e., aliased down into a range of periods over 2 pixels in length). In addition, the magnitude of the noise peak in the Fourier magnitude plot is listed.

A cursory look at Tables C-1 through C-6 may not reveal any relationship between the frequencies of the various coherent noise peaks. However, a closer look at the frequencies of the larger noise peaks reveals a definite relationship between these frequencies. For example, in the North Carolina data set, the four largest peaks occur at frequencies of 0.09, 2.20, 2.28 and 4.47 cycles/pixel. We note that 0.09 is approximately the difference between 2.28 and 2.20, and that 4.47 is approximately the sum of 2.20 and 2.28. Similar relationships between four of the larger noise peaks can also be found in the other data sets. (These sum and difference relationships are probably approximate only because of the discreteness of the frequency axis of the Fourier magnitude plots.)

Table C-1
Landsat-D Integrating Sphere Observed Coherent Noise
Frequency Peaks

Frequency		Aliased Period in Image Domain (pixels)	Fourier Magnitude (average)
(cycles/ (4096 samples))	(cycles/pixel)		
3	0.02	50	0.07
183	1.12	8.3	0.03
189	1.15	6.6	0.03
208	1.27	3.7	0.04
372	2.27	3.7	0.15
375	2.29	3.5	0.06
536	3.27	3.7	0.04
561	3.42	2.4	0.06
744	4.54	2.2	0.03
747	4.56	2.3	0.07
928	5.66	2.9	0.03
933	5.69	3.2	0.05
1114	6.80	5.0	0.03
1119	6.83	5.9	0.04
1300	7.93	14	0.06
1305	7.97	33	0.05
1491	9.10	10	0.03
1672	10.21	4.8	0.06
1680	10.25	4.0	0.04
1858	11.34	2.9	0.04
2044	12.48	2.1	0.03

An even more detailed look at the data reveals that, if sufficiently high harmonics are considered, almost all of the noise peaks are harmonically related to each other. To see this, we must remember that harmonics at frequencies higher than the "Nyquist" frequency (in this case, 12.5 cycles/pixel) appear in the Fourier magnitude plots as "alias" frequencies. For example, the thirteenth harmonic of 1 cycle/pixel (13 cycles/pixel) would appear at 12 cycles/pixel (25-13 = 12), and the twenty-sixth harmonic (26 cycles/pixel) would appear at 1 cycle/pixel (26-25 = 1).

To see how this occurs in the Landsat MSS coherent noise data, consider the North Carolina data as an example. The largest peak in the North Carolina data set occurs at 2.28 cycles/pixel. We could take 2.28 cycles/pixel to be the fundamental frequency, and look for harmonics of 2.28 cycles/pixel in the data. However, we will find that many more noise peaks can be harmonically related if we consider 1.14 cycles/pixel to be the fundamental frequency and 2.28 cycles/pixel to be the *second* harmonic of the fundamental frequency.

Table C-2a
Landsat-D′ Integrating Sphere Observed Coherent Noise
Frequency Peaks (without RC filters)

Frequency		Aliased Period in Image Domain (pixels)	Fourier Magnitude
(cycles/ (4096 samples))	(cycles/pixel)		
31	0.19	5.3	0.08
133	0.81	5.3	0.02
154	0.94	17	0.03
216	1.32	3.1	0.05
370	2.26	3.8	0.08
401	2.45	2.2	0.07
523	3.19	5.3	0.03
564	3.44	2.3	0.02
585	3.57	2.3	0.02
708	4.32	3.1	0.02
739	4.51	2.0	0.02
770	4.70	3.3	0.09
893	5.45	2.2	0.04
955	5.83	5.9	0.05
1078	6.58	2.4	0.03
1140	6.96	25	0.04
1324	8.08	12.5	0.03
1632	9.96	25	0.03

Table C-2b
Landsat-D′ Integrating Sphere Observed Coherent Noise
Frequency Peaks (with RC filters)

Frequency		Aliased Period in Image Domain (pixels)	Fourier Magnitude
(cycles/ (4096 samples))	(cycles/pixel)		
33	0.20	5.0	0.02
369	2.25	4.0	0.04
402	2.45	2.2	0.02
772	4.71	3.4	0.02

Table C-3
Landsat-4 Louisiana Data Observed Coherent Noise
Frequency Peaks

Frequency		Aliased Period in Image Domain (pixels)	Fourier Magnitude (average)
(cycles/ (4096 samples))	(cycles/pixel)		
11	0.07	14	0.14
176	1.07	14	0.05
198	1.21	4.8	0.05
362	2.21	4.8	0.12
373	2.28	3.6	0.24
384	2.34	2.9	0.04
538	3.28	3.6	0.03
549	3.35	2.9	0.07
571	3.49	2.0	0.04
736	4.49	2.0	0.13
747	4.56	2.3	0.03
757	4.62	2.6	0.04
879	5.36	2.8	0.04
923	5.63	2.7	0.05
944	5.76	4.2	0.05
1109	6.77	4.3	0.08
1131	6.90	10	0.06
1296	7.91	11	0.08
1318	8.04	25	0.11
1504	9.18	5.6	0.05
1669	10.19	5.3	0.03
1691	10.32	3.1	0.08
1845	11.26	3.8	0.05
1878	11.46	2.2	0.06

Considering the third through the tenth harmonic of 1.14 cycles/pixel, we find no corresponding noise peaks. The tenth harmonic (11.4 cycles/pixel) is also the highest harmonic we can directly observe in the Fourier transform magnitude plot. The eleventh harmonic is at 12.54 cycles/pixel, which is 0.04 cycles/pixel higher than the Nyquist frequency. Thus, if we have a noise peak at the eleventh harmonic, it would appear at 12.50 - 0.04 = 12.46 cycles/pixel in the Fourier magnitude plot. Looking back at Table C-4, we see that we do indeed have a noise peak at 12.46 cycles/pixel. The twelfth harmonic at 13.68 cycles/pixel would appear as an alias frequency of (12.50 - (13.68 - 12.50)) = (25.00 - 13.68) = 11.32 cycles/pixel. We see no noise peak at 11.32 cycles/pixel in Table C-4, but we do see a noise peak at the thirteenth harmonic (25.00 - 14.82 = 10.18 cycles/pixel), and at the fifteenth (7.90 cycles/pixel), sixteenth (6.76 cycles/pixel), seventeenth (5.62 cycles/pixel), eighteenth (4.48 cycles/pixel), nineteenth (3.34 cycles/pixel), twentieth (2.20 cycles/pixel), and twenty-first (1.06 cycles/pixel) harmonics.

The twenty-second harmonic at 25.08 cycles/pixel would appear at an alias frequency of 0.08 cycles/pixel (25.08 - 25.00). This is very close in frequency to the large peak at 0.09 cycles/pixel. Similarly, we see noise peaks at the twenty-third harmonic (26.22 - 25.00 = 1.22 cycles/pixel), and the twenty-fourth (2.36 cycles/pixel), twenty-sixth (4.64 cycles/pixel), twenty-seventh (5.78 cycles/pixel), twenty-eighth (6.92 cycles/pixel), twenty-ninth (8.06 cycles/pixel), thirtieth (9.20 cycles/pixel), thirty-first (10.34 cycles/pixel), and thirty-second (11.48 cycles/pixel) harmonics.

The thirty-third harmonic is at 37.62 cycles/pixel, which would appear at an alias frequency of 12.38 cycles/pixel (50.00 - 37.62 = 12.38). This is very near the noise peak at 12.37 cycles/pixel. Similarly, we see noise peaks at the thirty-fourth harmonic (50.00 - 38.76 = 12.24 cycles/pixel), and at the thirty-fifth harmonic (10.10 cycles/pixel).

Table C-4
Landsat-4 North Carolina Data Observed Coherent
Noise Frequency Peaks

Frequency		Aliased Period in Image Domain (pixels)	Fourier Magnitude
(cycles/ (4096 samples))	(cycles/pixel)		
14	0.09	11	0.11
173	1.06	17	0.05
201	1.23	4.3	0.07
210	1.28	3.6	0.05
360	2.20	5.0	0.10
374	2.28	3.6	0.21
388	2.37	2.7	0.04
546	3.33	3.0	0.08
733	4.47	2.1	0.11
761	4.64	2.8	0.04
920	5.62	2.6	0.08
948	5.79	4.8	0.06
1107	6.76	4.2	0.07
1135	6.93	14	0.04
1294	7.90	10	0.06
1322	8.07	14	0.12
1509	9.21	4.8	0.04
1592	9.72	3.6	0.05
1653	10.09	11	0.05
1667	10.17	5.9	0.04
1696	10.35	2.9	0.07
1756	10.72	3.6	0.04
1840	11.23	4.3	0.04
1882	11.49	2.0	0.04
2027	12.37	2.7	0.05
2041	12.46	2.2	0.05

The only noise peaks that cannot be associated with harmonics of 35 or less of 1.14 cycles/pixel are the noise peaks at 1.28, 9.72, and 10.72 cycles/pixel. We see here that only 3 of 26 noise peaks cannot be related to each other in this way. (These peaks could be due to some other noise source.)

The harmonic relationships can be made even more exact if we take our fundamental frequency to be a best fit to all the inferred harmonics. The best fit fundamental frequency for the North Carolina data set is 1.1403 cycles/pixel.

Tables C-7 through C-12 show the inferred relationships among the noise peaks for all the data sets that we studied. The tables list the observed frequency, the inferred harmonic number, and the inferred frequency of which each observed frequency is an alias if it is indeed the inferred harmonic of the fundamental. The best fit fundamental frequencies are given in a footnote to the tables. In addition, the tables list the harmonic frequencies calculated by multiplying the harmonic number times the best fit fundamental frequency of the respective data sets. The largest mismatch between the calculated and inferred frequencies is 0.016 cycles/pixel (in Table C-8b). Of the 85 cases listed in the tables, only 10 have a mismatch of greater than 0.005 cycles/pixel. (The accuracy to which the 4096 point Fourier Transform can measure frequency is ± 0.003 cycle/pixel). The match with the observed data is too accurate to be purely coincidental.

Tables C-7 through C-12 also give a signal-mixing representation of the relationships among the Fourier frequencies of coherent noise peaks. All of the harmonically related noise frequencies can be represented as sums and differences of the fundamental frequency and another frequency. In the case of the North Carolina data set, the fundamental frequency

Table C-5
Landsat-4 Florida Data Observed Coherent
Noise Frequency Peaks

Frequency		Aliased Period in Image Domain (pixels)	Fourier Magnitude
(cycles/ (4096 samples))	(cycles/pixel)		
20	0.12	8.3	0.09
167	1.02	50	0.07
207	1.26	3.8	0.06
354	2.16	6.2	0.17
374	2.28	3.6	0.27
395	2.41	2.4	0.06
541	3.30	3.3	0.10
728	4.44	2.3	0.13
915	5.58	2.4	0.09
956	5.83	5.9	0.05
1102	6.73	3.7	0.07
1143	6.98	50	0.07
1289	7.87	7.7	0.06
1322	8.12	8.3	0.14
1643	10.03	33	0.07
1704	10.40	2.5	0.12
1891	11.54	2.2	0.06
2018	12.32	3.1	0.04
2038	12.44	2.3	0.06

Table C-6
Landsat-5 Florida Data Observed Coherent
Noise Frequency Peaks

Frequency		Aliased Period in Image Domain (pixels)	Fourier Magnitude (average)
(cycles/ (4096 samples))	(cycles/pixel)		
19	0.12	8.3	0.05
207	1.26	3.8	0.03
371	2.26	3.8	0.07
390	2.38	2.6	0.03
760	4.64	2.8	0.03
1595	9.74	3.8	0.02
1759	10.74	3.8	0.03

Table C-7
Landsat-D Integrating Sphere Data Inferred Relationships
Among the Frequencies of Coherent Noise Peaks in the Fourier
Magnitude Plots

Signal Mixing Representation*	Observed Frequency (cycles/pixel)	Inferred Harmonic Number	Freq. Inferred from Harmonic No. (cycles/pixel)	Harmonic No. × Fund Freq.* (cycles/pixel)
2A	2.27	2	2.27	2.271
4A	4.54	4	4.54	4.542
8A + B	9.10	14	15.90	15.898
7A + B	7.97	15	17.03	17.034
6A + B	6.83	16	18.17	18.170
5A + B	5.69	17	19.31	19.305
4A + B	4.56	18	20.44	20.441
3A + B	3.42	19	21.58	21.576
2A + B	2.29	20	22.71	22.712
A + B	1.15	21	23.85	23.848
B	0.02	22	24.98	24.983
A–B	1.12	23	26.12	26.119
5A–B	5.66	27	30.66	30.661
6A–B	6.80	28	31.80	31.797
7A–B	7.93	29	32.93	32.932
9A–B	10.21	31	35.21	35.204
10A–B	11.34	32	36.34	36.339
11A–B	12.48	33	37.48	37.475
9A + 2B	10.25	35	39.75	39.746
(A + 8B)	1.27	(175)	(198.73)	(198.730)
(3A–8B)	3.27	(179)	(203.27)	(203.272)

*Inferred fundamental frequency is 1.1356 cycles/pixel (114.04 kHz). For signal-mixing representation, A = 1.1356 cycles/pixel and B = 0.0168 cycles/pixel.

is A = 1.1403 cycles/pixel, and an appropriate "other" frequency is B = 0.0866 cycles/pixel. B is approximately equal to the observed frequency of the twenty-second harmonic. A-B is near the observed frequency of the twenty-first harmonic, and 2A-B is near the twentieth harmonic, etc. A + B is near the observed frequency of the twenty-third harmonic, and 2A + B is near the twenty-fourth harmonic, etc.

A number of different frequencies could be used as the "other" frequency in the signal-mixing representation. If we take C = 2A + B, then the twenty-fourth harmonic equals C, the twenty-third equals C-A, the twenty-second equals C-2A, the twenty-first equals 3A-C, and the twentieth harmonic equals 4A-C, etc.

Table C-13 lists the inferred fundamental frequencies from Tables C-7 through C-12. Note that the fundamental frequencies all fall within the nominal frequency range given for the MSS power supply switching frequency (110 ± 5 kHz).

Table C-8a
Landsat-D′ Integrating Sphere Data (without RC filter) Inferred Relationships Among the Frequencies of Coherent Noise Peaks in the Fourier Magnitude Plots

Signal Mixing Representation*	Observed Frequency (cycles/pixel)	Inferred Harmonic Number	Freq. Inferred from Harmonic No. (cycles/pixel)	Harmonic No. × Fund Freq. * (cycles/pixel)
2A	2.26	2	2.26	2.256
4A	4.51	4	4.51	4.511
7A + B	8.08	15	16.92	16.917
6A + B	6.96	16	18.04	18.045
5A + B	5.83	17	19.17	19.173
4A + B	4.70	18	20.30	20.300
3A + B	3.57	19	21.43	21.428
2A + B	2.45	20	22.55	22.556
A + B	1.32	21	23.68	23.684
B	0.19	22	24.81	24.812
A–B	0.94	23	25.94	25.939
3A–B	3.19	25	28.19	28.195
4A–B	4.32	26	29.32	29.323
5A–B	5.45	27	30.45	30.451
6A–B	6.58	28	31.58	31.578
9A–B	9.96	31	34.96	34.962
?	0.81	?	?	?
?	3.44	?	?	?

*Inferred fundamental frequency is 1.1278 cycles/pixel (113.26 kHz). For signal-mixing representation, A = 1.1278 cycles/pixel and B = 0.1884 cycles/pixel.

Table C-8b
Landsat-D′ Integrating Sphere Data (with RC Filter) Inferred Relationships Among the Frequencies of Coherent Noise Peaks in the Fourier Magnitude Plots

Signal Mixing Representation*	Observed Frequency (cycles/pixel)	Inferred Harmonic Number	Freq. Inferred from Harmonic No. (cycles/pixel)	Harmonic No. × Fund Freq. * (cycles/pixel)
2A	2.25	2	2.25	2.253
4A + B	4.71	18	20.29	20.281
2A + B	2.45	20	22.55	22.534
B	0.20	22	24.80	24.787

*Inferred fundamental frequency is 1.1267 cycles/pixel (113.15 kHz). For signal-mixing representation, A = 1.1267 cycles/pixel and B = 0.2126 cycles/pixel.

Table C-9
Landsat-4 Louisiana Data Inferred Relationships Among the
Frequencies of Coherent Noise Peaks in the Fourier Magnitude Plots

Signal Mixing Representation*	Observed Frequency (cycles/pixel)	Inferred Harmonic Number	Freq. Inferred from Harmonic No. (cycles/pixel)	Harmonic No. × Fund Freq.* (cycles/pixel)
2A	2.28	2	2.28	2.279
4A	4.56	4	4.56	4.558
9A–B	10.19	13	14.81	14.813
7A–B	7.91	15	17.09	17.092
6A–B	6.77	16	18.23	18.231
5A–B	5.63	17	19.37	19.371
4A–B	4.49	18	20.51	20.510
3A–B	3.35	19	21.65	21.649
2A–B	2.21	20	22.79	22.789
A–B	1.07	21	23.93	23.928
B	0.07	22	25.07	25.068
A + B	1.21	23	26.21	26.207
2A + B	2.34	24	27.34	27.347
3A + B	3.49	25	28.49	28.486
4A + B	4.62	26	29.62	29.626
5A + B	5.76	27	30.76	30.765
6A + B	6.90	28	31.90	31.904
7A + B	8.04	29	33.04	33.044
8A + B	9.18	30	34.18	34.183
9A + B	10.32	31	35.32	35.323
10A + B	11.46	32	36.46	36.462
10A–2B	11.26	34	38.74	38.741
3A–2B	3.28	41	46.72	46.717
(5A–5B)	5.36	(105)	(119.64)	(119.637)

*Inferred fundamental frequency is 1.1394 cycles/pixel (114.42 kHz). For signal-mixing representation, A = 1.1394 cycles/pixel and B = 0.0668 cycles/pixel.

Table C-10
Landsat-4 North Carolina Data Inferred Relationships Among
the Frequencies of Coherent Noise Peaks in the Fourier Magnitude Plots

Signal Mixing Representation*	Observed Frequency (cycles/pixel)	Inferred Harmonic Number	Freq. Inferred from Harmonic No. (cycles/pixel)	Harmonic No. × Fund Freq. * (cycles/pixel)
2A	2.28	2	2.28	2.281
11A–B	12.46	11	12.54	12.543
9A–B	10.17	13	14.83	14.824
7A–B	7.90	15	17.10	17.104
6A–B	6.76	16	18.24	18.245
5A–B	5.62	17	19.38	19.385
4A–B	4.47	18	20.53	20.525
3A–B	3.33	19	21.67	21.666
2A–B	2.20	20	22.80	22.806
A–B	1.06	21	23.94	23.946
B	0.09	22	25.09	25.087
A + B	1.23	23	26.23	26.227
2A + B	2.37	24	27.37	27.367
4A + B	4.64	26	29.64	29.648
5A + B	5.79	27	30.79	30.788
6A + B	6.93	28	31.93	31.928
7A + B	8.07	29	33.07	33.069
8A + B	9.21	30	34.21	34.209
9A + B	10.35	31	35.35	35.349
10A + B	11.49	32	36.49	36.490
11A–2B	12.37	33	37.63	37.630
10A–2B	11.23	34	38.77	38.770
9A–2B	10.09	35	39.91	39.910
(8A + 7B)	9.72	(162)	(184.72)	(184.729)
(10A–8B)	10.72	(166)	(189.28)	(189.290)
?	1.28	?	?	?

*Inferred fundamental frequency is 1.1403 cycles/pixel (114.51 kHz). For signal-mixing representation, A = 1.1403 cycles/pixel and B = 0.0866 cycles/pixel.

Table C-11
Landsat-4 Florida Data Inferred Relationships Among the
Frequencies of Coherent Noise Peaks in the Fourier Magnitude Plots

Signal Mixing Representation*	Observed Frequency (cycles/pixel)	Inferred Harmonic Number	Freq. Inferrfed from Harmonic No. (cycles/pixel)	Harmonic No. × Fund. Freq. * (cycle/pixel)
2A	2.28	2	2.28	2.284
11A-B	12.44	11	12.56	12.561
7A-B	7.87	15	17.13	17.129
6A-B	6.73	16	18.27	18.270
5A-B	5.58	17	19.42	19.412
4A-B	4.44	18	20.56	20.554
3A-B	3.30	19	21.70	21.696
2A-B	2.16	20	22.84	22.838
A-B	1.02	21	23.98	23.980
B	0.12	22	25.12	25.121
A + B	1.26	23	26.26	26.264
2A + B	2.41	24	27.41	27.406
5A + B	5.83	27	30.83	30.831
6A + B	6.98	28	31.98	31.973
7A + B	8.12	29	33.12	33.115
9A + B	10.40	31	35.40	35.399
10A + B	11.54	32	36.54	36.541
11A-2B	12.32	33	37.68	37.683
9A-2B	10.03	35	39.97	39.967

*Inferred fundamental frequency is 1.1419 cycles/pixel (114.67 kHz). For signal-mixing representation, A = 1.1419 cycles/pixel and B = 0.1218 cycles/pixel.

Table C-12
Landsat-5 Florida Data Inferred Relationships Among the
Frequencies of Coherent Noise Peaks in the Fourier Magnitude Plots

Signal Mixing Representation*	Observed Frequency (cycles/pixel)	Inferred Harmonic Number	Freq. Inferred from Harmonic No. (cycles/pixel)	Harmonic No. × Fund Freq.* (cycles/pixel)
2A	2.26	2	2.26	2.261
4A + B	4.64	18	20.36	20.353
2A + B	2.38	20	22.62	22.614
A + B	1.26	21	23.74	23.745
B	0.12	22	24.88	24.875
?	9.74	?	?	?
?	10.74	?	?	?

*Inferred fundamental frequency is 1.1307 cycles/pixel (113.55 kHz). For signal-mixing representation, A = 1.1307 cycles/pixel and B = 0.1246 cycles/pixel.

Table C-13
Inferred Fundamental Frequencies

Data Set	Cycles/Pixel	Frequency (kHz)
Integrating Sphere (Landsat-D)	1.1356	114.04
Integrating Sphere (Landsat-D′)		
(without RC filter)	1.1278	113.26
(with RC filter)	1.1267	113.15
Louisiana, Lake Pontchartrain (Landsat-4)	1.1394	114.42
North Carolina, Atlantic Ocean (Landsat-4)	1.1403	114.51
Florida, Gulf of Mexico (Landsat-4)	1.1419	114.67
Florida, Gulf of Mexico (Landsat-5)	1.1307	113.55

APPENDIX D

PLOTS OF FILTERS USED IN FILTERING LANDSAT-4 MSS COHERENT NOISE FROM THE NORTH CAROLINA DATA SET

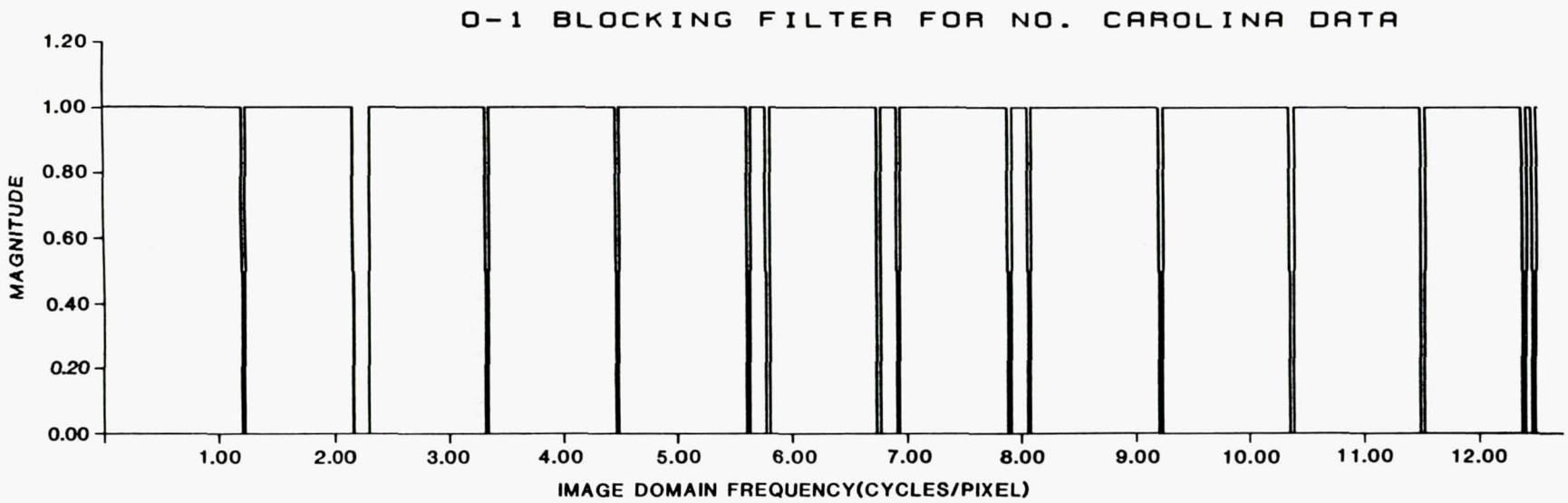

Figure D-1. Frequency domain plot of the 0 - 1 blocking filter for the North Carolina data set. Only the positive, nonnegative frequency components are displayed.

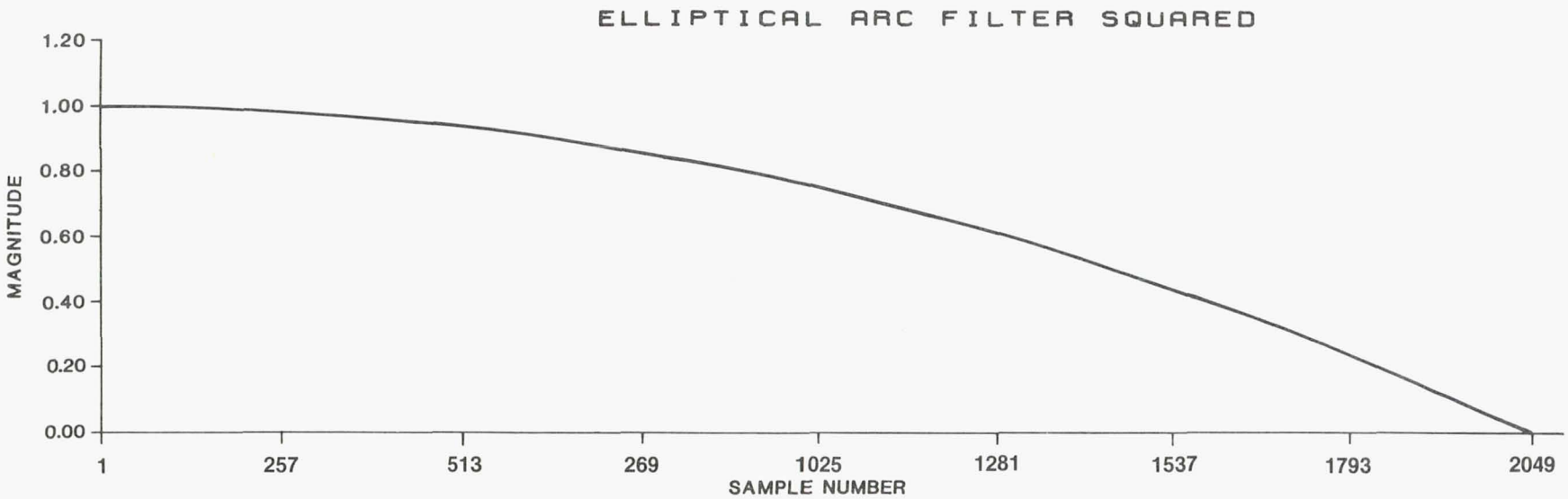

Figure D-2. Spatial domain plot of the elliptical arc squared filter used for "rounding" the 0 - 1 blocking filter. The lower half of the plot is shown; the upper half is the mirror image of the lower half.

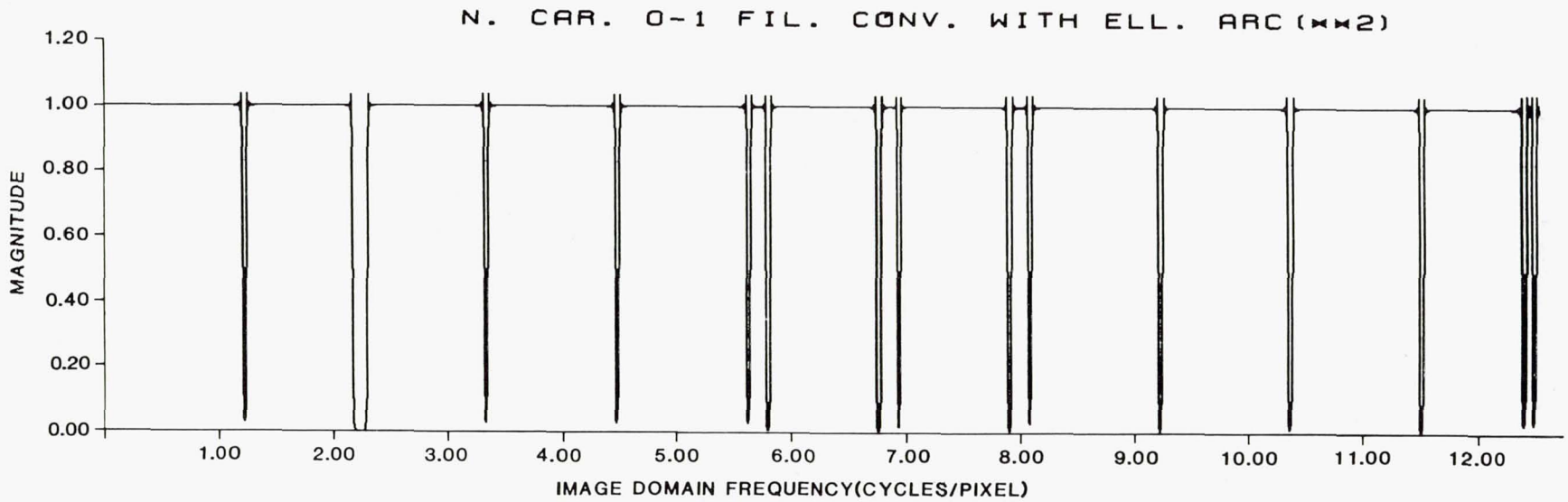

Figure D-3. Frequency domain plot of the "rounded" 0 - 1 blocking filter for the North Carolina data set. Only the positive, nonnegative frequency components are displayed.

NASA
National Aeronautics and Space Administration

Report Documentation Page

1. Report No.	2. Government Accession No.	3. Recipient's Catalog No.
NASA TP-2595 Revised		

4. Title and Subtitle	5. Report Date
Landsat-4 and Landsat-5 Multispectral Scanner Coherent Noise Characterization and Removal	February 1988
	6. Performing Organization Code: 630
7. Author(s): James C. Tilton and William L. Alford	8. Performing Organization Report No.: 86B0040
	10. Work Unit No.
9. Performing Organization Name and Address: Goddard Space Flight Center, Greenbelt, Maryland 20771	11. Contract or Grant No.
	13. Type of Report and Period Covered: Technical Paper
12. Sponsoring Agency Name and Address: National Aeronautics and Space Administration, Washington, D.C. 20546-0001	14. Sponsoring Agency Code

15. Supplementary Notes

William L. Alford is affiliated with the Defense Mapping Agency, HQ/STT, Washington, D.C., 20305.

16. Abstract

This report describes a technique for characterizing the coherent noise found in Landsat-4 and Landsat-5 MSS data and a companion technique for filtering out the coherent noise. The techniques are demonstrated on Landsat-4 and Landsat-5 MSS data sets, and explanations of the noise pattern are suggested in Appendix C. A cookbook procedure for characterizing and filtering the coherent noise using special NASA/Goddard IDIMS functions is included in Appendix A. Presented also are analysis results from the retrofitted Landsat-5 MSS sensor, which shows that the coherent noise has been substantially reduced.

17. Key Words (Suggested by Author(s))	18. Distribution Statement
Landsat Multispectral Scanner (data acquisition); Remote sensing of Earth resources; Computer processing of Earth resources data	Unclassified - Unlimited Subject Category 43

19. Security Classif. (of this report)	20. Security Classif. (of this page)	21. No. of pages	22. Price
Unclassified	Unclassified	52	A04

NASA FORM 1626 OCT 86